MASARYKOVA UNIVERZITA

PŘÍRODOVĚDECKÁ FAKULTA

Nanočástice pro detekci acetylcholinesterasy

Diplomová práce

ONDŘEJ ŠABACKÝ

Vedoucí práce: doc. RNDr. Petr Skládal, CSc.

Ústav biochemie

Specializace: Analytická biochemie

Brno 2021

Bibliografický záznam

Autor:	Ondřej Šabacký Přírodovědecká fakulta Masarykova univerzita Ústav biochemie
Název práce:	Nanočástice pro detekci acetylcholinesterasy
Studijní program:	Biochemie
Specializace:	Analytická biochemie
Vedoucí práce:	doc. RNDr. Petr Skládal, CSc.
Rok:	2021
Počet stran:	66
Klíčová slova:	acetylcholinesterasa, inhibitory acetylcholinesterasy, elektrochemie, stříbrné nanočástice, ITO

Bibliographic record

Author:	Ondřej Šabacký Faculty of Science Masaryk University Department of Biochemistry
Title of Thesis:	Nanoparticles for detection of acetylcholinesterase
Degree Programme:	Biochemistry
Specialization:	Analytical biochemistry
Supervisor:	doc. RNDr. Petr Skládal, CSc.
Year:	2021
Number of Pages:	66
Keywords:	acetylcholinesterase, acetylcholinesterase inhibitors, electrochemistry, silver nanoparticles, ITO

Abstrakt

Tato diplomová práce se zabývá problematikou stanovení inhibitorů acetylcholinesterasy (AChE) pomocí biosenzorů s AChE imobilizovanou na jejich povrchu. Jako modelový inhibitor byl použit eserin (physostigmin).

V praktické části byly nejdříve stanoveny amperometrické odezvy na ITO (cínem dopovaný oxid inditý) páscích a platinových elektrodách s imobilizovanou AChE s použitím substrátu acetylthiocholinu (ATCh). Dále byly připraveny stříbrné nanočástice stabilizované citrátem sodným a draselným (citrate-capped AgNPs) a jejich velikost stanovena pomocí mikroskopie atomárních sil (AFM). Tyto nanočástice byly využity pro stanovení inhibice AChE vyvolané agregační reakcí. Průběh agregace těchto nanočástic byl také ověřen pomocí Ramanovy spektroskopie.

Nakonec byly u platinových elektrod s imobilizovanou AChE pomocí cyklické voltametrie (CV) stanoveny rozdíly v odezvách na různé koncentrace inhibitoru eserinu.

Abstract

This diploma thesis deals with the determination of acetylcholinesterase (AChE) inhibitors using biosensors with surface-immobilized AChE. Eserine (physostigmine) was used as a model inhibitor.

In the practical part, amperometric responses for ITO (indium tin oxide) strips and platinum electrodes with surface-immobilized AChE were first determined using acetylthiocholine substrate (ATCh). Furthermore, silver nanoparticles stabilized with sodium and potassium citrate (citrate-capped AgNPs) were prepared, and their size was characterized using atomic force microscopy (AFM). These nanoparticles were further used for the determination of AChE inhibition triggered by aggregation reaction. The course of aggregation of these nanoparticles was also verified by Raman spectroscopy.

Finally, for platinum electrodes with surface-immobilized AChE, differences in responses to different concentrations of eserine inhibitor were determined by cyclic voltammetry (CV).

MUNI
SCI

MASARYKOVA UNIVERZITA
PŘÍRODOVĚDECKÁ FAKULTA
KOTLÁŘSKÁ 2, 611 37 BRNO
IČ: 00216224
DIČ: CZ00216224

ZADÁNÍ DIPLOMOVÉ PRÁCE

Akademický rok: 2020/2021

Ústav:	Ústav biochemie
Student:	Bc. Ondřej Šabacký
Program:	Biochemie
Specializace:	Analytická biochemie

Ředitel *ústavu* PřF MU Vám ve smyslu Studijního a zkušebního řádu MU určuje diplomovou práci s názvem:

Název práce:	Nanočástice pro detekci acetylcholinesterasy
Název práce anglicky:	Nanoparticles for detection of acetylcholinesterase
Jazyk závěrečné práce:	angličtina

Oficiální zadání:
Klasické stanovení aktivity acetylcholinesterasy (AChE) využívá hydrolytické štěpení acetylcholinu a redoxní reakci vzniklého thiocholinu s Elmanovým činidlem za vzniku žlutého zbarvení; fotometrické měření přitom nepatří mezi nejcitlivější. Mnohem nižší aktivity lze přitom stanovit s využitím nanočástic stříbra (Ag NP). Thiocholin může sloužit k jejich tvorbě či následné agregaci, což lze výhodně sledovat. Cílem práce bude porovnat jednotlivé strategie spojení AChE s Ag NP detekcí, vybrat 1 až 2 systémy a ty pak porovnat v kombinovaném měření na bázi průhledné ITO elektrody. Bude tak možné paralelně sledovat elektrické změny (impedance, voltametrie) či optickou odezvu (změna fluorescence či barvy). Optimalizovaný systém bude vyzkoušen pro stanovení inhibitorů AChE (insekticidy, léčiva) a nebo spřažen s modelovým imunosensorem využívajícím AChE jako značku.

Literatura

Xia N. Nanomaterials-Based Optical Techniques for the Detection of Acetylcholinesterase and Pesticides. Sensors 2015, 15, 499-514.
Li Z. Unmodified silver nanoparticles for rapid analysis of the organophosphorus pesticide, dipterex, often found in different waters. Sensors and Actuators B 2014, 193, 205-211.
Liu R. Application of gold–silver nanocluster based fluorescent sensors for determination of acetylcholinesterase activity and its inhibitor. Materials Research Express, 2018, 5, 065027.
Kumar ND. Acetylcholinesterase (AChE)-mediated immobilization of silver nanoparticles for the detection of organophosphorus pesticides RSC Advances 2016, 6, 64769-64777.

Vedoucí práce:	doc. RNDr. Petr Skládal, CSc.
Datum zadání práce:	15. 10. 2019
V Brně dne:	13. 5. 2021

Zadání bylo schváleno prostřednictvím IS MU.

Bc. Ondřej Šabacký, 18. 3. 2021
doc. RNDr. Petr Skládal, CSc., 14. 4. 2021
RNDr. Jitka Kašparovská, Ph.D., 11. 5. 2021

Acknowledgments

I would like to express my gratitude to doc. RNDr. Petr Skládal, CSc. for his help, patience, willingness, and valuable advice he provided me with during the creation of this work. I would also like to express my appreciation to Ing. Jakub Máčala and Mgr. Matěj Pastucha for their help with practical experiments.

Declaration

Prohlašuji, že jsem svoji práci vypracoval samostatně pod vedením vedoucího práce s využitím informačních zdrojů, které jsou v práci citovány.

Brno May 31, 2021 .....

Ondřej Šabacký

Table of Contents

GLOSSARY **12**

1 INTRODUCTION **13**

2 ACETYLCHOLINESTERASE **14**

2.1 Determination of the activity of AChE 18

2.2 Inhibition of AChE 19

2.3 Inhibitors of AChE 20

2.3.1 Reversible AChE inhibitors 20

2.3.2 Irreversible AChE inhibitors (organophosphorus compounds) 22

3 SILVER NANOPARTICLES (AGNPS) **24**

4 INDIUM TIN OXIDE (ITO) **25**

5 BIOSENSORS **26**

5.1 Definition of the biosensor 26

5.2 History of biosensors 26

5.3 Physical-chemical converter 27

5.4 Basic concepts 28

5.5 Enzyme immobilization 29

6 ELECTROCHEMICAL METHODS **30**

6.1 Amperometry 31

6.2 Cyclic voltammetry 31

7 AIMS AND OBJECTIVES **33**

8 MATERIALS AND METHODS **34**

8.1 Apparatus 34

8.2 Reagents 36

8.3 Methodology 37

8.3.1 Preparation of phosphate-buffered saline (PBS) 37

8.3.2 Synthesis of citrate-capped AgNPs 37

8.3.3 Immobilization of AChE on ITO-coated PET foil 37

8.3.4 Immobilization of AChE on platinum electrodes (AC1.W2.RS) 38

8.3.5 Amperometric measurements 38

8.3.6 Cyclic voltammetry measurements 40
8.3.7 Spectrophotometric measurements 41
8.3.8 AFM analysis of citrate-capped AgNPs 41
8.3.9 Raman spectroscopy analysis of citrate-capped AgNPs 41

9 RESULTS AND DISCUSSION 42

9.1 Results of amperometric measurements with platinum electrodes 42
9.2 Results of amperometric measurements with ITO strips 47
9.3 CV measurements with platinum electrodes 52
9.4 Spectrophotometric measurements of citrate-capped AgNPs 54
9.5 AFM 57
9.6 Raman spectroscopy 60

10 CONCLUSION 62

11 BIBLIOGRAPHY 63

List of Figures and Tables

Figure 1 – Native AChE from Torpedo californica. [2] 14
Figure 2 – AChE from Electrophorus electricus (tetramer). [4] 15
Figure 3 – AChE at the synaptic cleft. [6].....17
Figure 4 – Mechanism of AChE-catalyzed hydrolysis of ACh. [1].....18
Figure 5 – General structure of biologically active carbamates. [1] 22
Figure 6 – General structure of OPs. [1] 23
Figure 7 – Structural formulas of selected nerve agents and DDVP. [11] 24
Figure 8 – Schematic illustration of the novel analysis of organophosphorus pesticides (OPs) based on the inhibition of an enzyme and the use of the aggregation process of citrate-capped AgNPs. [16] 25
Figure 9 – Cyclic voltammetry. [26] 32
Figure 10 – USB Potentiostat EmStat. 34
Figure 11 – Amperometric sensor AC1.W2.RS. 34
Figure 12 – Spectrophotometer NanoPhotometer® NP 80.....35
Figure 13 – Diagram of measuring apparatus. 39
Figure 14 – Diagram of measuring apparatus. 40
Figure 15 – Amperometric response to ATCh. 43
Figure 16 – Amperometric response to ATCh. 44
Figure 17 – Amperometric response to ATCh. 45
Figure 18 – Amperometric responses to ATCh all in one graph. 46
Figure 19 – Amperometric responses ATCh on an electrode without immobilized enzyme (control). 46
Figure 20 – Connection of the flow cell using crocodile clips. 47
Figure 21 – Amperometric response to an addition of 1 mM ATCh on an ITO strip with surface-immobilized AChE (1 nkat μl^{-1}). Potential 600 mV. 48
Figure 22 – Amperometric response to an addition of 1 mM ATCh on an ITO strip with surface-immobilized AChE (1 nkat μl^{-1}). Potential 700 mV. 48
Figure 23 – Amperometric response to an addition of 1 mM ATCh on an ITO strip with surface-immobilized AChE (1 nkat μl^{-1}). Potential 800 mV. 49
Figure 24 – Amperometric response to an addition of 1 mM ATCh on an ITO strip with surface-immobilized AChE (1 nkat μl^{-1}). Potential 1000 mV. 49

Figure 25 – Amperometric response to an addition of 1 mM ATCh on an ITO strip with surface-immobilized AChE (0.1 nkat μl^{-1}). Potential 800 mV. 50
Figure 26 – Amperometric response to an addition of 1mM ATCh on an ITO strip with surface-immobilized AChE (0.01 nkat μl^{-1}). Potential 800 mV. 51
Figure 27 – CV response to ATCh/$AgNO_3$ mixture. 52
Figure 28 – CV response to ATCh/$AgNO_3$ mixture (various inhibitor concentrations). 53
Figure 29 – Current at 0.8 V (top half-wave) against eserine concentrations.....54
Figure 30 – Citrate-capped AgNPs prepared using sodium citrate. 55
Figure 31 – Citrate-capped AgNPs prepared using potassium citrate. 55
Figure 32 – Recorded spectra for solutions prepared using AgNPs prepared with sodium citrate. 56
Figure 33 – Recorded spectra for solutions prepared using AgNPs prepared with potassium citrate. 57
Figure 34 – AFM images of citrate-capped AgNPs (sodium citrate). 58
Figure 35 – AFM images of citrate-capped AgNPs (sodium citrate). 58
Figure 36 – AFM images of citrate-capped AgNPs (potassium citrate). 59
Figure 37 – AFM images of aggregated AgNPs (potassium citrate – left, sodium citrate –right). 59
Figure 38 – SERS of fresh and aggregated AgNPs. 60

Table I – Responses to additions of ATCh (AChE 0.01 nkat μl^{-1}).....43
Table II – Responses to additions of ATCh (AChE 0.1 nkat μl^{-1}).....44
Table III – Responses to additions of ATCh (AChE 1 nkat μl^{-1}).....45
Table IV – Responses to additions of ATCh (AChE 1 nkat μl^{-1}). 50
Table V – Responses to additions of ATCh.....51
Table VI – Intensity at 1590 cm^{-1}. 60

Glossary

4-MBA	4-Mercaptobenzoic acid
ACh	Acetylcholine
AChE	Acetylcholinesterase
AD	Alzheimer's disease
AFM	Atomic force microscopy
AgNP(s)	Silver nanoparticles
APTES	(3-Aminopropyl)triethoxysilane
ATCh	Acetylthiocholine (chloride)
CV	Cyclic voltammetry
EA	Ethanolamine
ITO	Indium tin oxide (coated PET)
OPs	Organophosphorus compounds
PBS	Phosphate-buffered saline
SERS	Surface-enhanced Raman spectroscopy

1 Introduction

Determination of the activity and inhibition of acetylcholinesterase is a powerful tool in medical diagnostics of several neurodegenerative diseases, as well as pesticide and nerve agent intoxication. Although Ellman's method has been widely used to determine acetylcholinesterase activity, it has limits, especially for field use.

With the increasing use of pesticides based on acetylcholinesterase inhibitors, the need arises for a simple and compact device capable of detection thereof. Transparent ITO electrodes (ITO-coated pet foil) or the corundum ceramic-based platinum electrodes combined with immobilized acetylcholinesterase could serve well for this purpose.

Furthermore, attention has recently turned to silver nanoparticles for their electrochemical and surface plasmon resonance properties. Therefore, silver nanoparticles could act as signal enhancers for the electrochemical biosensors with surface-immobilized acetylcholinesterase. In addition, silver nanoparticles can also be used for the spectrophotometrical determination of acetylcholinesterase inhibition.

This thesis deals with the preparation of a biosensor capable of detecting acetylcholinesterase inhibition while using silver nanoparticles as response signal enhancers.

2 Acetylcholinesterase

Acetylcholinesterase (AChE, EC 3.1.1.7) is an enzyme of the hydrolases class found in various sorts of electric impulse conducting tissue: nerve and muscle, central and peripheral tissues, motor and sensory fibers, and cholinergic and noncholinergic fibers. The activity of AChE is higher in motor neurons than in sensory neurons. [1]

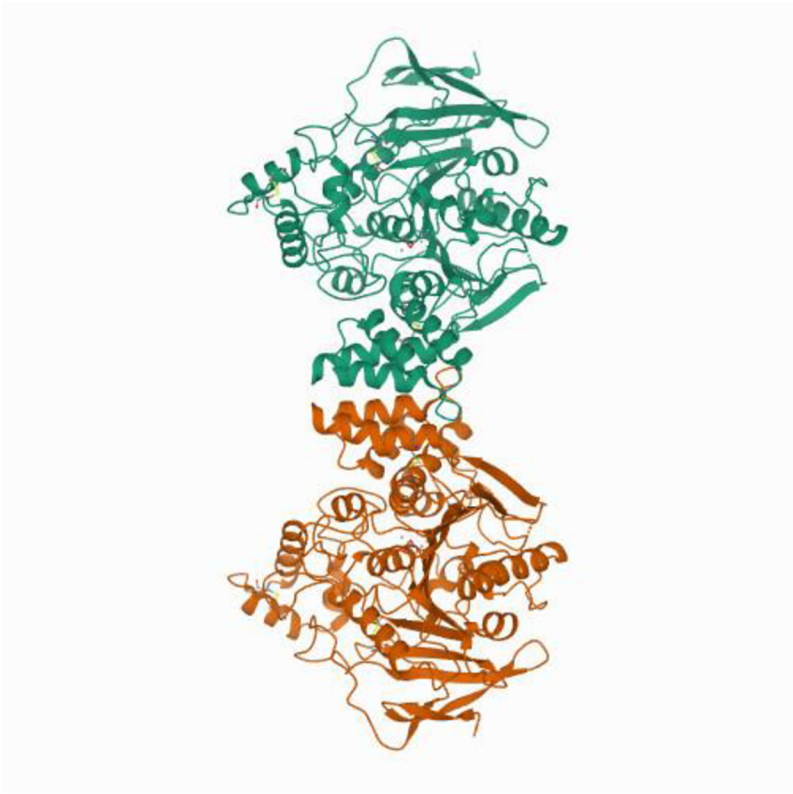

Figure 1 – Native AChE from *Torpedo californica.* [2]

This cholinergic enzyme instantly degrades or hydrolyzes acetylcholine (ACh), a neurotransmitter present in many living organisms, including humans, to acetic acid and choline (Equation 1). The primary purpose of AChE is to end neuronal transmission and signaling between synapses to prevent ACh from spreading and the activation of nearby receptors. AChE is inhibited by organophosphates and carbamates, which are an essential component of pesticides and nerve agents. [3]

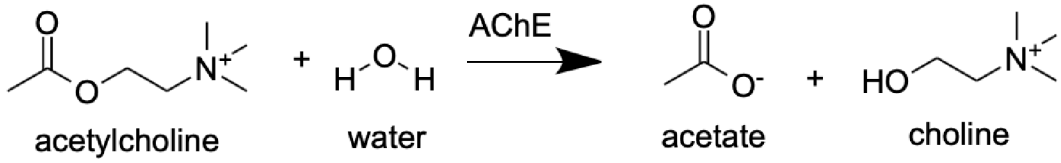

Equation 1 – AChE-catalyzed hydrolysis of ACh.

AChE is a monomer that often forms a disulfide bond dimer. Thanks to Van der Waals forces, two dimers can be further joined into tetramers. The tetramers group and bind themselves to what is described as "tails" composed of three chains. From a chemical and immunological point of view, the structure of these tails resembles the structure of collagen, and thus they can be disintegrated by collagenases. With another disulfide bond, the tetramer dimers associate with each tail. [3]

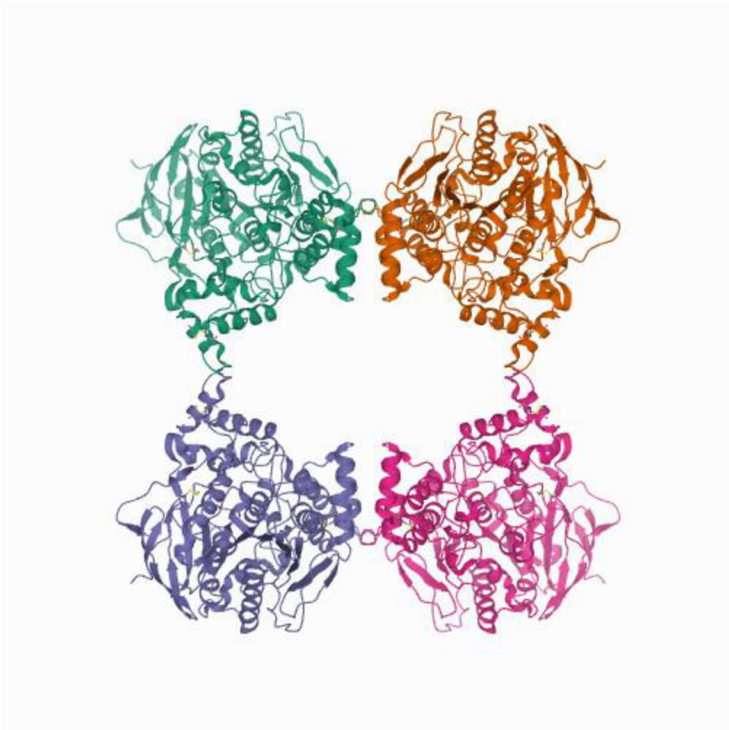

Figure 2 – AChE from *Electrophorus electricus* (tetramer). [4]

The active site of AChE consists of two subsites: the anionic and esteratic subsites. The anionic subsite serves as the binding site for the positively charged quaternary amine of ACh. The esteratic subsite is the place where ACh becomes hydrolyzed to acetate and choline. [5]

The main role of AChE is the termination of neural transmission. However, AChE is also crucial for neural development. AChE is intricately involved in the embryological development of the nervous system and is expressed by developing neurons and during periods of axonal growth (a time in which enzymatic activity does not seem to be most important). Transient AChE activity was locally present in the dorsal root ganglions in the peripheral nervous system of chicks. These discoveries suggest that AChE, in addition to its primary enzymatic function, contributes to morphogenesis during fetal development. [3]

AChE is known to be distributed in nervous tissue such as the brainstem, cerebellum, peripheral, and autonomic nervous systems. Skeletal muscles also contain AChE with distribution patterns seemingly related to the type of muscle (fast versus slow-twitch) and their specific function. [3]

Less commonly known is the presence and function of AChE on red blood cells. Blood group antigens are found on the outer lipid bilayer of red blood cells, which serves for convenient antibody recognition. Similarly, AChE is present on red blood cell membranes as well. [3]

The neurotransmitter ACh is released when a neural signal propagates and excites or activates a cellular membrane. The ACh receptor then undergoes a conformational change, and the membrane releases calcium ions. These calcium ions play a role in exciting the fibers of nerves and muscles by triggering an additional change in phospholipids. Essentially, the downstream effect of a signal initiated with ACh results in amplification and propagation of the cellular signaling. [3]

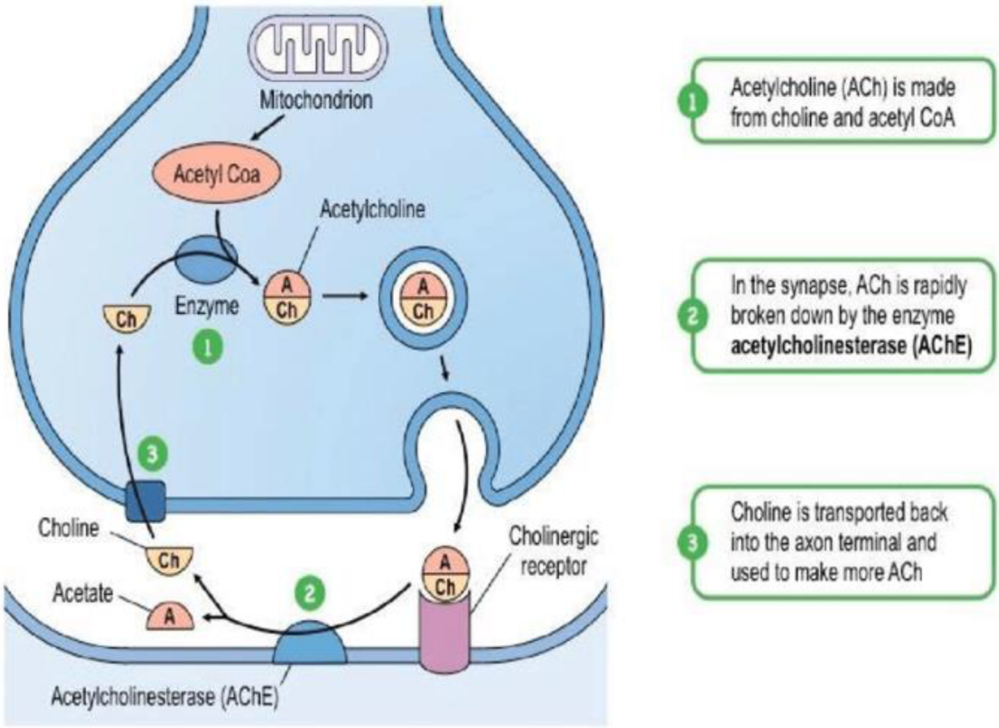

Figure 3 – AChE at the synaptic cleft. [6]

The interaction of AChE with the substrate ACh results in its breakdown, hydrolysis, inactivation, and subsequent control of the amount of ACh at the synapse. AChE is a serine hydrolase that creates a tetrahedral intermediate through acid-base reactions with a catalytic triad (serine 200, histidine 440, glutamate 327). Histidine allows for the transference of a proton between the serine and ACh oxygen molecules, thereby removing choline to form a new acylated serine. The regeneration of free AChE begins when the acylated serine is deacylated. Aspartate stabilizes the protonated histidine, leading to acetic acid and a new, free enzyme release. The interaction between amino acid residues (tyrosine, phenylalanine, tryptophan) that make up a peripheral anionic site influences the conformational binding of ACh to that site. [3]

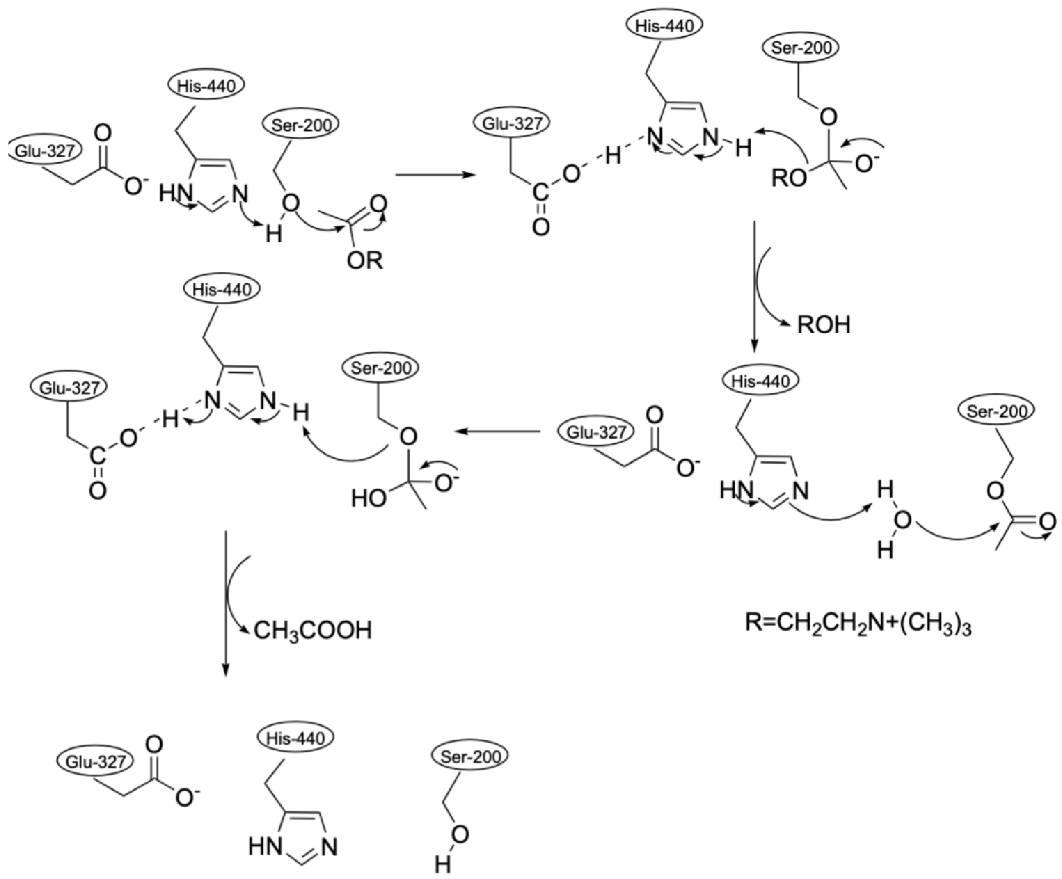

Figure 4 – Mechanism of AChE-catalyzed hydrolysis of ACh. [1]

2.1 Determination of the activity of AChE

Knowledge of the current state of cholinesterase activity in the body is crucial for the early diagnosis of organophosphate intoxication and monitoring the effectiveness of administered therapy, especially AChE reactivators. Erythrocyte AChE is most commonly used for this assay, as it is readily available, and its degree of inhibition corresponds very well to the severity of poisoning. [7]

Many methodologies have been developed to determine cholinesterase activity. The most commonly used methods are electrometric, titration, colorimetric, determination of pH change using an indicator, spectrophotometric, fluorimetric, radiometric, polarographic, and enzyme. However, the methods mentioned above cannot be introduced into routine practice for many reasons, such as sample pre-treatment, long measurement times, or insufficient substrate specificity of the enzyme. [7]

A susceptible and suitable method for everyday use was described by Ellman. This colorimetric method is now used to evaluate the health status of people who generally come into contact with organophosphorus inhibitors (industrial and agricultural workers). [7]

The principle of this method is based on the hydrolysis of acetylthiocholine. After enzymatic hydrolysis, acetic acid and thiocholine are released. Thiocholine containing the SH group in its molecule is detected by 5,5'-dithiobis-2-nitrobenzoic acid (DTNB) by releasing the yellowish 5-mercapto-2-nitrobenzoate anion (TNB^-) after the reaction with thiocholine. This anion is then detected spectrophotometrically at a wavelength of 412 nm. [7]

Although the Ellman's method is fast, cheap, and straightforward, it also has its disadvantages. Interference with hemoglobin is very crucial in measuring blood cholinesterase activities. The absorption maximum of the color indicator TNB^- is 412 nm. However, the hemoglobin present in the blood also absorbs radiation at this wavelength. If we want to rule out such an error, a blood sample has to be significantly diluted. Another problem is the reaction of Ellman's reagent (DTNB) with slow-reacting sulfhydryl groups in the solution, which can affect the measurement results. [7]

These shortcomings have led to many modifications to the original Ellman method. For example, to reduce interference with hemoglobin, two-beam spectrophotometers or other chromogenic disulfides have been used to measure different wavelengths. Another way to improve the determination of AChE in the blood is to use selective BChE (butyrylcholinesterase) inhibitors such as either quinidine or phenothiazine derivatives. [7]

2.2 Inhibition of AChE

Inhibition of hydrolysis of ACh leads to serious health risks. Inhibition or alteration of AChE activity may occur for several reasons. Reduced levels of the neurotransmitter ACh in the body lead to neurodegenerative diseases such as Alzheimer's disease, Parkinson's disease, or Huntington's disease. Another reason for reduced enzyme activity may be a disorder of proteosynthesis or an inherited defect, e.g., familial idiopathic acholinesterasemia. AChE may also be inhibited by inactivation. The inhibitor (pesticide, nerve agent) binds to the hydroxyl group of serine at the active

site of AChE, thereby preventing the breakdown of ACh to acetate and choline in the synaptic cleft. As a result of inhibition, excess ACh accumulates in the tissues, and signal transmission is interrupted, resulting in muscle weakness, muscle paralysis, seizures in the CNS, impaired neuromuscular disc function, and, in severe cases, respiratory problems, fibrillation, and death. [8]

2.3 Inhibitors of AChE

AChE inhibitors inhibit the ability of cholinesterase to decompose ACh, thereby increasing the concentration of neurotransmitter and duration of action. AChE inhibitors are usually divided into two groups based on their mode of action: irreversible and reversible. Reversible inhibitors, both competitive and non-competitive, find application in therapy. Irreversible AChE inhibitors, on the other hand, have toxic effects. [1]

2.3.1 Reversible AChE inhibitors

Reversible AChE inhibitors play an essential role in the pharmacological manipulation of enzyme activity. These inhibitors include compounds with different functional groups (carbamate, quaternary or tertiary ammonium group) and have been used to diagnose and treat various diseases such as myasthenia gravis, AD, postoperative ileus, bladder distension, glaucoma, as well as antidotes for anticholinergic overdose. [1]

Alzheimer's disease treatment using reversible AChE inhibitors

Alzheimer's disease (AD) is the most common cause of dementia and accounts for up to 80 % of all dementia diagnoses. [9] AD is a progressive neurological disorder characterized by loss of memory and other intellectual abilities severe enough to interfere with daily life. The disease is associated with the loss of cholinergic neurons in the brain and decreased ACh levels. Inhibition of cerebral AChE is a primary therapeutic target in AD treatment strategies. There is no cure for AD, and the reversible AChE inhibitors used in therapy treat the symptoms associated with memory, thinking, language, judgment, and other thought consequences. Various

physiological processes related to AD damage or cell destruction that produce and use ACh, thereby reducing the amount of ACh available for message delivery to other cells. Cholinesterase inhibitor drugs that inhibit AChE activity maintain ACh levels by reducing the rate of AChE degradation. Consequently, they increase cholinergic neurotransmission in areas of the forebrain and compensate for the loss of functional brain cells. However, no drug indicates delaying or stopping the progression of the disease. Drugs that are currently approved by regulatory agencies, such as the US Food and Drug Administration (FDA) and the European Medicines Agency (EMA), to treat cognitive manifestations of AD and improve patients' quality of life are donepezil, rivastigmine, and galantamine, such as are reversible inhibitors of AChE and memantine as NMDA receptor antagonists. Tacrine was the first AChE inhibitor approved for AD treatment in 1993, but its use was discontinued due to a high incidence of adverse events, including hepatotoxicity. [1]

Carbamates

Carbamates are organic compounds derived from carbamic acid (NH_2COOH). Carbamate compounds find use in human medicine as therapeutic drugs (AD, myasthenia gravis, glaucoma, Lewy bodies, Parkinson's disease). In addition, these reversible AChE inhibitors have been applied as pesticides and parasiticides in veterinary medicine and prophylaxis of organophosphorus compounds (OPs) poisoning. [1]

Carbamates, unlike organophosphorus pesticides, have a relatively quick decarbamylation step which means that substantial recovery of the enzyme can occur in a finite period of time. [5] Figure 5 shows a biologically active carbamate structure, where X can be oxygen or sulfur (thiocarbamate), R_1 and R_2 are usually organic or alkyl substituents, but R_1 or R_2 may also be hydrogen, and R_3 is primarily an organic substituent or sometimes a metal. [1]

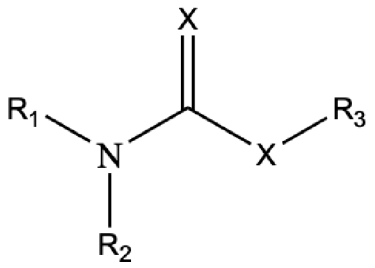

Figure 5 – General structure of biologically active carbamates. [1]

Carbamates have a similar toxicological presentation to OP poisonings with a duration of toxicity that is typically less than 24 hours. Common agents resulting in toxic exposure are aldicarb, carbofuran, carbaryl, ethinenocarb, fenobucarb, oxamyl, methomyl, pirimicarb, propoxur, and trimethacarb. [10]

2.3.2 Irreversible AChE inhibitors (organophosphorus compounds)

Organophosphorus compounds (OPs) are either oxones or thiones derived from phosphoric, phosphonic, phosphinic, or phosphoramidic acid (Figure 6). R_1 and R_2 are aryl or alkyl groups bonded to the phosphorus atom either directly (forming phosphinates) or through an oxygen or sulfur atom (forming phosphates or phosphothioates). R_1 might sometimes be directly bonded to the phosphorus atom, and R_2 is bonded to an oxygen or sulfur atom (forming phosphonates or thiophosphonates). In phosphoramidates, at least one of these groups is $–NH_2$ (un-, mono- or bi-substituted), and the atom double-bonded with phosphorus is either oxygen or sulfur. Also binding to the phosphorus atom through oxygen or sulfur atom is the –X group, which may be halogen, aliphatic, aromatic, or heterocyclic groups. This leaving group is released from the phosphorus atom when the OP is hydrolyzed by phosphotriesterases or upon interaction with protein targets. In medicine and agriculture, the word "organophosphates" refers to a group of insecticides and nerve agents that inhibit AChE. [1]

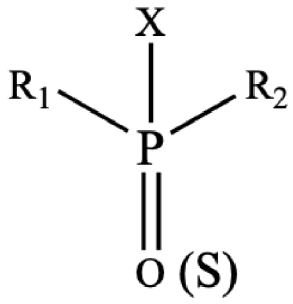

Figure 6 – General structure of OPs. [1]

OP pesticides such as diazinon, dichlorvos (DDVP), parathion, and paraoxon are widely used in modern agriculture to protect crops from pests and insects. [11] [12] However, the OP-induced contamination of agricultural products, environments, and even foods has raised increasing public concerns. It has been reported that OPs can cause neurotoxic poisoning to both animals and humans because of their strong ability to irreversibly block the activity of AChE in cholinergic synapses and neuromuscular junctions at very low concentrations, resulting in the accumulation of ACh throughout the body and, thus, exerting a malignant influence on human health with severe consequences. Therefore, reliable and sensitive analytical methods for detecting OPs in trace levels have become increasingly important. Many sensitive analytical methods, including colorimetric assays, fluorescence methods, photoelectrochemical approaches, photonic sensing platforms, and liquid crystal sensing platforms, have been established to detect OPs. Many of these OP assay methods rely on the mechanism of AChE-catalyzed hydrolysis of the artificial substrate acetylthiocholine (ATCh) due to its high sensitivity and rapid response. Although these reported methods showed satisfactory results for OP analysis, it is still attractive to achieve higher sensitivity. [13] Biosensor techniques based on the inhibition of AChE activity have lately gained considerable attention due to benefits, such as simplicity, rapidity, reliability, and low-cost instrumentation. Different AChE-based amperometric, potentiometric, or optical biosensors have been reported. In amperometric AChE-based biosensors, enzyme inhibition is monitored by the change in the oxidation current of thiocholine at a specific potential. Nanomaterials have also been employed to make electrochemical biosensors with improved analytical performance. [14] In recent years, surface-enhanced Raman spectroscopy (SERS) has been considered a tool for OP detection. [15]

Besides being used as pesticides, OPs are also used as potent nerve agents, namely, sarin, soman, tabun, cyclosarin, and VX.

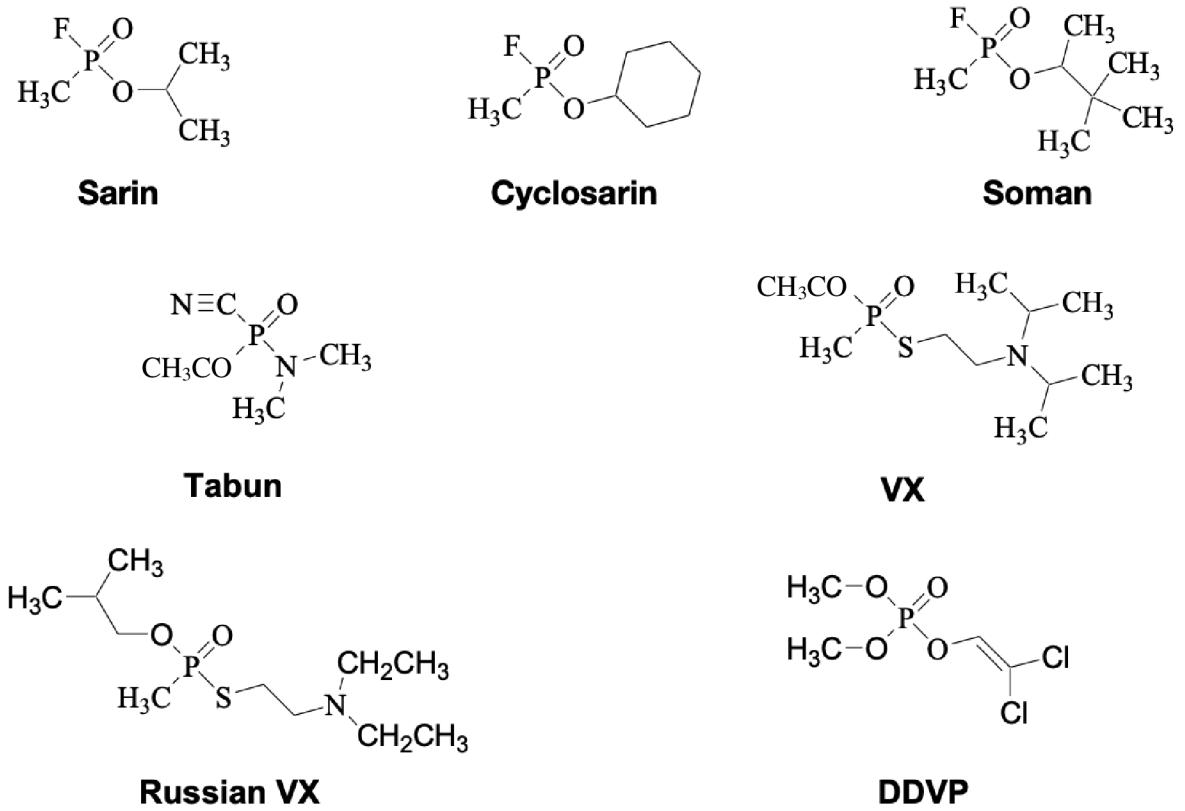

Figure 7 – Structural formulas of selected nerve agents and DDVP. [11]

3 Silver nanoparticles (AgNPs)

The practical use of noble metal nanoparticles (NPs) for biological and biomedical applications is widely explored due to their strong surface plasmon resonance (SPR). The metallic NPs possess unique physical, chemical, and biological properties due to their nanometer-size range and shape. The unique optical properties of gold and silver NPs result from their strong absorption and scattering of light. Among other NPs, AgNPs have been utilized in surface-enhanced Raman scattering (SERS), plasmonic absorbance, catalysis, antimicrobials, and biosensors. AgNPs are often used combined with biologically active molecules that can pass on the response to toxic chemical agents. Several studies have reported the rapid and direct detection of AChE inhibitors in aqueous solutions by sensitive and straightforward colorimetric

AChE-based assays using NPs. AuNPs and AgNPs are widely used for OP pesticide detection in environmental and biological systems due to their distinct color properties. Therefore, AgNPs have been receiving significant interest in recent years in the field of novel biosensors and as a very efficient support matrix for enzyme immobilization. Enzyme immobilization on NPs can lower protein unfolding, which increases the enzyme stability (and activity) and biosensor performance. [12] Enzyme-catalyzed deposition of AgNPs can also serve to enhance the response signal output. [13]

AgNPs can be prepared using a citric acid salt as a stabilizing agent. Such AgNPs (citrate-capped) can be used in the spectrophotometric determination of AChE inhibition. A synthetic substrate, acetylthiocholine (ATCh), is hydrolyzed to thiocholine (TCh), which induces the aggregation of AgNPs, leading to a color change (Figure 8). [16]

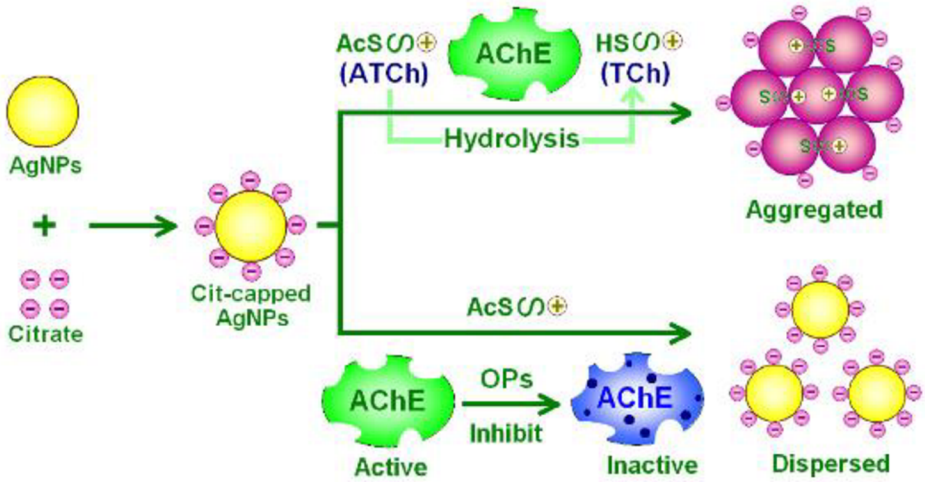

Figure 8 – Schematic illustration of the novel analysis of organophosphorus pesticides (OPs) based on the inhibition of an enzyme and the use of the aggregation process of citrate-capped AgNPs. [16]

4 Indium Tin Oxide (ITO)

The first transparent conductive thin film of oxide was prepared from cadmium oxide, and it is not used anymore due to its toxicity. Later on, a thin film of tin dioxide was prepared in 1937 and a thin film of indium oxide in 1954. [17]

Indium tin oxide (ITO) is a composition of indium oxide and tin dioxide in a ratio of 9:1. It is one of the most widely used transparent and, at the same time, conductive

thin films based on metal oxides. Transparent conductive oxide thin films have, as the name suggests, good electrical conductivity and low light absorption, but also good substrate adhesion, low capacitive current, and stable electrochemical and physical properties. These properties make them ideal for the production of biosensors and electrodes and electrodes in photovoltaic devices. [18]

ITO thin films are prepared by various techniques, such as electron beam evaporation, radiofrequency magnetron sputtering, chemical deposition of vapors, and the most commonly used chemical deposition from solution due to its simplicity and low cost. [17][19]

5 Biosensors

5.1 Definition of the biosensor

For the first time, the biosensor was defined by G. Rechnitz as an analytical instrument consisting of an immobilized biorecognition component and a physicochemical transducer. [20] The biorecognition part recognizes the analyte by two basic principles - biocatalytic (tissue, cell, enzyme), where the analyte is a substrate of the enzyme reaction, and bioaffinity (antibody, receptor, nucleic acid, lectin), where the analyte is bound in an affinity complex. The physical-chemical transducer of which the bio-cognition part is a part or is in close contact with it provides a final electronic analytical signal proportional to the concentration of the analyte or group of substances. [21]

IUPAC (International Union of Pure and Applied Chemistry) defines a biosensor as: "A device that utilizes specific biochemical interactions mediated by isolated enzymes, immunosystems, tissues, organelles, or whole cells to detect chemical compounds, usually by electrical, thermal, or optical signals." [22]

5.2 History of biosensors

At the beginning of the journey to biosensors was Leland C. Clark Jr. and his discovery of the oxygen sensor. Clark separated the working platinum electrode from

the sample with a gas-permeable membrane and moved the reference electrode behind the membrane, creating the sensor itself. [23]

Thanks to this discovery, there was a massive development of biosensors with immobilized enzyme on the membrane. If there is dissolved oxygen on the side of the reactants or products, the sensor makes it possible to measure the loss or increase of oxygen, which is directly proportional to the concentration of analyte = substrate. [23]

The first commercially successful biosensor was a blood glucose biosensor. Yellow Spring Instruments introduced a commercially available enzyme electrode for the determination of blood glucose in 1975. In 1987, the introduction of GlucoPen ExacTech became an essential milestone for people with diabetes. [21]

We currently encounter many biosensors used in clinical diagnostics, the military, agriculture, food, sports, and other industries. [21]

5.3 Physical-chemical converter

A physical-chemical transducer is a system that converts changes arising from specific biochemical reactions into a measurable electrical signal suitable for further evaluation. Depending on the type of biocatalyst, the correct type of transducer must be selected.

In principle, the converters can be divided into the following groups:

- Optical
- Electrochemical
- Piezoelectric and acoustic
- Electromagnetic
- Calorimetric

The most often encountered are electrochemical converters, mainly due to low production and acquisition costs, simple construction, and high sensitivity. [21]

5.4 Basic concepts

Sensitivity – a stable change in the output signal caused by a change in the analyte concentration. Ideally, the sensitivity should be constant; in practice, recalibration is necessary.

Calibration – measuring the response using standard solutions of known concentration.

Linearity – ideally in the entire work area. In practice, this is a narrower interval within the work area.

Detection limit – this is the smallest possible detectable analyte concentration.

Noise – most often electromagnetic, can be prevented by shielding the sensor and wires. It can also be caused by turbulence in a stirred arrangement.

Background signal – generated in the absence of analyte, usually read automatically.

Hysteresis – is caused by previous measurements on the current signal. It manifests itself by a change in the shape of the calibration curves, on which concave or convex motion can be observed.

Long-term stability – depends on changes in the sensitivity of the biosensor over time. The decrease in sensitivity may be due to oxidation of the surface or deposition of layers of molecules on the surface of the biosensor.

Selectivity – ideally, the signal should change only after the addition of the test substance. In practice, it is necessary to eliminate substances causing interference (e.g., by a selective barrier) or to determine their share in the total signal by another sensor at the same time.

Response rate – depends on the physical properties, especially the rate of diffusion from the environment to the surface of the biosensor and then to diffusion within the biosensor system.

Response time – the time required to reach a specific constant signal size.

The convection rate – is determined by the supply of substances from the environment. It can be accelerated by agitation or flow of the medium, but excessive speed, which could lead to turbulent phenomena, must be avoided.

Temperature dependence – affects the ongoing reaction and diffusion. The solution is to work in an isothermal environment or monitor temperature.

Service life is given by the lifespan of the biorecognition part. A lower temperature is usually suitable for long-term storage. Appropriate conditions vary for each biosensor.

Biocompatibility is essential when working in living tissues - treatment against blood clotting and disinfection. [21]

5.5 Enzyme immobilization

It is necessary to properly attach the biorecognition component to the transducer to ensure the correct functioning of biosensors. This process is called immobilization, and five basic methods are distinguished:

Adsorption

This fast and straightforward method uses adsorbent materials such as graphite, alumina, cellulose, or silica gel. Enzymes are weakly bound to the material, which is a disadvantage. This method is suitable for short-term use. The material is sensitive to changes in temperature and pH.

Encapsulation

The biorecognition component is located behind the inert membrane, where it is in close contact with the transducer. This method is reliable and flexible, stable to changes in temperature and pH. It is used in the glucose biosensor.

Capture

The biorecognition component is mixed with the monomer solution and then polymerized into a gel. The biological sample is then retained in the gel. Polyacrylamide is usually used for capture. The problem is the slow diffusion of the substrate and the associated longer measurement time.

Cross-linking

Glutaraldehyde is usually used to capture the biorecognition component on a solid surface. The advantage is the possibility of stabilizing the adsorbed enzyme. However, enzyme damage and reduced substrate diffusion may occur. In addition, the method does not show good resistance to mechanical influences.

Covalent bond

A covalent bond is formed between the functional group and the transducer or membrane. The enzyme is attached tightly. The reaction conditions must be mild. [14]

6 Electrochemical methods

Electrochemistry deals with processes in systems containing charged particles. For example, electrochemical methods are often used to measure the catalytic activity of enzymes. It is prevalent mainly due to the simple construction of the electrochemical system, low acquisition costs, and high sensitivity. The electrochemical measuring system must contain at least a working and a reference electrode. [21] Today, modern technology allows the construction of microscopic systems, for example, by screen

printing. There are several electrochemical methods. This thesis further deals with amperometry and cyclic voltammetry (CV).

6.1 Amperometry

Amperometry works on the principle of monitoring the current that arises during the oxidation or reduction of an electroactive substance. The current is usually measured at a constant voltage at the working electrode. The current generated during a reaction over a given period indicates a charge that is proportional to the concentration of analytes converted on the electrodes. The measurement is most often performed in a two-electrode arrangement, where the voltage on the working electrode is set against the auxiliary electrode. Another possibility is to measure in a three-electrode arrangement, in which there is also a reference electrode. The voltage of the working electrode is set against the reference electrode. The benefit of the three-electrode arrangement lies in the elimination of the effect of the magnitude of the current in the solution on the voltage at the working electrode. Thanks to this, it is possible to achieve a much higher current value using a three-electrode system compared to a two-electrode arrangement. Therefore, the three-electrode system is more versatile, but a potentiostat is required for its operation. [21]

6.2 Cyclic voltammetry

CV is an electrochemical technique that measures the current that develops in an electrochemical cell under conditions where voltage is more than that predicted by the Nernst equation. CV is performed by cycling the potential of the working electrode and measuring the resulting current. [24]

The basic principle of CV is step changes of potential in time, from maximum to minimum value (forward scan) and backward (reverse scan). The breakpoint is called E_s. A typical voltammetric curve of a reversible redox process can be described from an electrochemical point of view as follows: by gradually changing the potential from maximum to minimum, a reduction occurs until the maximum cathodic current is reached (at that moment, the further current increase limits the transport of substance to the surface of the electrode) at the potential of E_{pc}. As the rate of loss of oxidized

form of the substance increases, its amount around the electrode decreases, and once there is too little of the substance, the current gradually decreases, while the potential decreases to the point E_s. At that moment, the direction of potential growth changes, and the reverse process gradually begins (oxidation of the accumulated reduced form). There is a gradual increase in the reduced form of the analyte, and the maximum anodic current is reached. After exceeding the E_{pa} potential to which this maximum corresponds, there is not enough of the reduced form of the substance around the electrode that could be oxidized, and the current gradually decreases until the system returns to its initial state at maximum potential (Figure 9). In the field of biosensors, this method is of great importance, especially in the study of new electrochemical systems. [21][25]

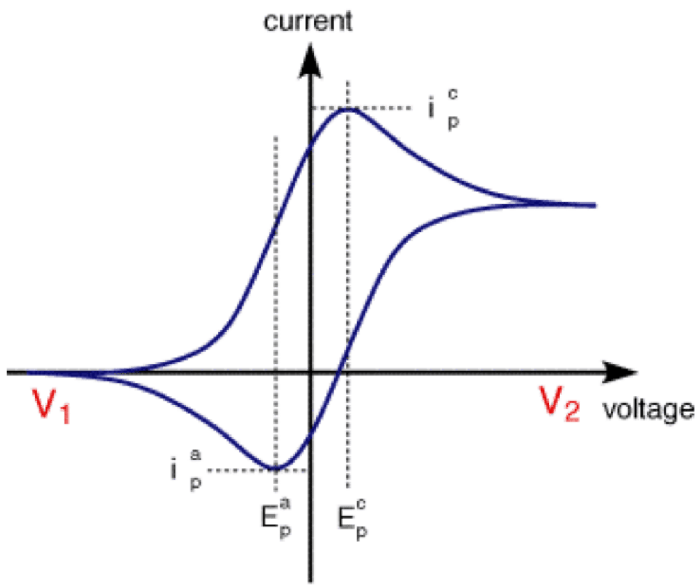

Figure 9 – Cyclic voltammetry. [26]

7 Aims and Objectives

1. Immobilization of AChE on ITO strips and platinum sensors.
2. Preparation of citrate-capped AgNPs.
3. Determination of the size and physical properties of prepared nanoparticles.
4. Amperometric determination of response to ATCh substrate on prepared sensors with surface-immobilized AChE.
5. Determination of AChE inhibition using CV and spectrophotometrical methods combined with AgNPs.

8 Materials and methods

8.1 Apparatus

USB potentiostat EmStat

- Manufacturer: Palmsens BV, The Netherlands
- Measurable current range: 1 nA – 100 mA
- Associated with PSTrace software

Figure 10 – USB Potentiostat EmStat.

Amperometric sensor AC1.W2.RS

- Manufacturer: BVT Technologies, a.s., Czechia
- Dimensions: 25.4 × 7.26 × 0.63 mm
- Working electrode: platinum (Pt)
- Base: corundum ceramic

Figure 11 – Amperometric sensor AC1.W2.RS.

Spectrophotometer NanoPhotometer® NP 80

- Manufacturer: Implen GmbH, Germany

- Wavelength range: 200 nm – 900 nm
- Sample: cuvette, drop

Figure 12 – Spectrophotometer NanoPhotometer® NP 80.

Atomic force microscope (AFM) Dimension FastScan Bio

- Manufacturer: Bruker Co., USA
- Probe: Scanasyst-Air, tip height: 2.5-8 μm
- Image processing software: NanoScope Analysis

Raman Spectrometer AvaRaman

- Manufacturer: Avantes, The Netherlands
- Laser probe: 532 nm
- processing software: Avasoft 8

Other devices:

- Analytical balance Scaltec SBC 22, Germany
- Electromagnetic stirrer Color squid, IKA, Germany
- Peristaltic pump Miniplus 3, Gilson, USA
- pH meter inoLab pH 720 equipped with SenTix 21 pH electrode, Germany

8.2 Reagents

- Acetone, 58.08 g mol^{-1}, supplied from: Penta, Czech Republic
- AChE (Acetylcholinesterase from *Electrophorus electricus* (electric eel), EC 3.1.1.7), lyophilized powder, 200-1 000 units/mg protein, manufacturer: Sigma-Aldrich, USA
- $AgNO_3$ (Silver nitrate), 169.87 g mol^{-1}, manufacturer: Penta, Czechia
- APTES ((3-Aminopropyl)triethoxysilane), 221.37 g mol^{-1}, manufacturer: Sigma-Aldrich, USA
- ATCh (Acetylthiocholine chloride), 197.73 g mol^{-1}, manufacturer: Sigma-Aldrich, USA
- Cystamine dihydrochloride, 225.20 g mol^{-1}, manufacturer: Sigma-Aldrich, USA
- Ethanolamine, 61.08 g mol^{-1}, manufacturer: Sigma-Aldrich, USA
- Glutaraldehyde, 50% water solution, 100.12 g mol^{-1}, manufacturer: Sigma-Aldrich (Fluka), USA
- ITO (Indium tin oxide) coated PET, 100 Ω/sq, manufacturer: Sigma-Aldrich, USA
- 4-MBA (4-Mercaptobenzoic acid), 154.19 g mol^{-1}, manufacturer: Sigma-Aldrich, USA
- $NaBH_4$ (Sodium borohydride), 37.83 g mol^{-1}, manufacturer: Ubichem, UK
- NaCl (Sodium chloride), 58.44 g mol^{-1}, manufacturer: Penta, Czechia
- $NaH_2PO_4 \cdot 2H_2O$ (Sodium phosphate monobasic dihydrate), 156.01 g mol^{-1}, manufacturer: Penta, Czechia
- PBS (50mM phosphate, 150mM NaCl, pH = 7,4)
- Eserine (Physostigmine), 387.4 g mol^{-1}, provided by Petr Skládal
- Potassium citrate, 306.40 g mol^{-1}, manufacturer: Chemapol, Czechia
- Sodium citrate, 258.06 g mol^{-1}, Penta, Czechia

8.3 Methodology

8.3.1 Preparation of phosphate-buffered saline (PBS)

The PBS was prepared with 50 mM NaH_2PO_4 and 150 mM NaCl, weighed quantities were dissolved in an appropriate volume of distilled water, and then the pH was adjusted to a final value of 7.4 with 1 mM NaOH solution.

8.3.2 Synthesis of citrate-capped AgNPs

The citrate-capped AgNPs were prepared according to Z. Li et al. First, 250 µl of 100 mM $AgNO_3$ solution was added to 100 ml of distilled water in a beaker in a cold-water bath (~5 °C) while stirring vigorously. Then, 250 µl of 100mM sodium citrate solution and 6 ml of 5 mM sodium borohydride ($NaBH_4$) solution were sequentially added to the solution. $NaBH_4$ reduces Ag^+ ions to Ag^0 atomic silver. $NaBH_4$ in the presence of sodium citrate also forms AgNPs, with the citrate salt acting as the stabilizing agent. The instant color change from colorless to light yellow indicated the creation of dispersed, colloidal AgNPs. The AgNP mixture was stirred vigorously for another 30 minutes. The resulting product was then stored in the refrigerator at 5 °C for further use. [16]

Another batch of colloidal citrate-capped AgNPs was prepared using a slightly modified procedure when the 100 mM sodium citrate solution was substituted with 100 mM potassium citrate solution. Similar results were obtained with potassium citrate solution.

8.3.3 Immobilization of AChE on ITO-coated PET foil

AChE was immobilized on 3 × 1 cm ITO-coated PET foil strips. The strips were cut to desired dimensions using scissors. The first step was to wash the strips in acetone for at least 10 minutes. The strips were then silanized by immersing in 2% APTES solution (0.2 ml of APTES, 9.8 ml of acetone) for 1 hour. After the incubation in APTES solution, the strips were then washed with acetone and dried. In the next step, the strips were incubated in 3% glutaraldehyde solution in PBS for 1 hour. After

this step, the strips were washed with distilled water, dried and 70 µl of AChE solution of the desired activity (1 nkat μl^{-1}, 0.1 nkat μl^{-1}, and 0.01 nkat μl^{-1}) were then applied on each strip. The strips placed in a sealed Petri dish to avoid evaporation of AChE solution were stored in a refrigerator overnight.

On the other day, the AChE solution was washed off with distilled water, and the strips were incubated in a 1% solution of aminoethanol in PBS for 30 minutes. Then the strips were washed with distilled water, dried, and stored dry in a sealed Petri dish in the refrigerator.

8.3.4 Immobilization of AChE on platinum electrodes (AC1.W2.RS)

AChE was immobilized on AC1.W2.RS corundum ceramic-based platinum electrodes. The first step was to wash the electrodes in acetone for at least 10 minutes. After drying, 2 µl of 10 mg ml^{-1} cystamine distilled water solution was added onto each working electrode for 1 hour. After the incubation solution, the electrodes were washed with distilled water and dried. In the next step, 2 µl of 3% glutaraldehyde solution in PBS was added onto each working electrode for 1 hour. After this step, the electrodes were washed with distilled water, dried, and 2 µl of AChE solution of the desired activity (1 nkat μl^{-1}, 0.1 nkat μl^{-1}, and 0.01 nkat μl^{-1}) were then applied on each electrode. The electrodes placed in a sealed Petri dish to avoid evaporation of AChE solution were stored in a refrigerator overnight.

The next day, the AChE solution was washed off with distilled water, and the electrodes were washed with distilled water, dried, and stored dry in a sealed Petri dish in the refrigerator.

8.3.5 Amperometric measurements

Amperometric measurements were carried out in mixed as well as flow arrangements at positive potentials ranging from 300 mV to 800 mV.

For amperometric measurements in the mixed arrangement, the AC1.W2.RS electrodes with surface-immobilized AChE were immersed in a beaker containing 10 ml of PBS and connected to the EmStat potentiostat. The content of the beaker was stirred at a constant speed of 300 rpm using an electromagnetic stirrer. The

chronoamperometry method was selected in the PSTrace software, and the potential was set to 300 mV. After the background signal stabilization, four volumes of 10 µl, 20 µl, 20 µl, and 50 µl of 100 mM acetylthiocholine (ATCh) solution were sequentially added to the stirred PBS. It was essential to wait for the signal stabilization between each addition of the ATCh solution. These steps were repeated for each sensor with different AChE activities used for the immobilization (1 nkat μl^{-1}, 0.1 nkat μl^{-1}, and 0.01 nkat μl^{-1}).

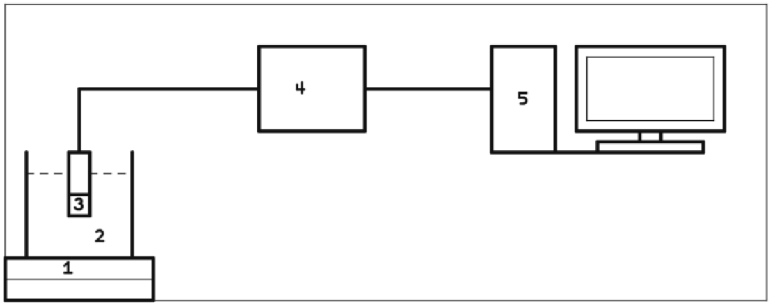

Figure 13 – Diagram of measuring apparatus.

1 - the electromagnetic stirrer, 2 - beaker with a working solution, 3 - electrochemical sensor AC1.W2.RS, 4 - potentiostat EmStat, 5 - a desktop computer with PSTrace software.

For amperometric measurements in the flow arrangement, the ITO strips with surface-immobilized AChE were placed in a flow cell connected to a peristaltic pump. The cell contained electrodes that were in contact with the ITO strip. The cell was connected to the potentiostat using crocodile clips. The chronoamperometry method was selected in the PSTrace software, and the potential was set from 600 mV to 1000 mV.

First, PBS was pumped into the cell at 2.5 rpm (approx 60 µl min^{-1}). Then, after the background signal stabilization, 1 mM ATCh solution was pumped into the cell at 2.5 rpm. It was again necessary to wait for the signal stabilization. Then, PBS was pumped into the cell at 2.5 rpm again. These steps were repeated for both potentials and each ITO strip with different AChE activity (1 nkat μl^{-1}, 0.1 nkat μl^{-1}, and 0.01 nkat μl^{-1}).

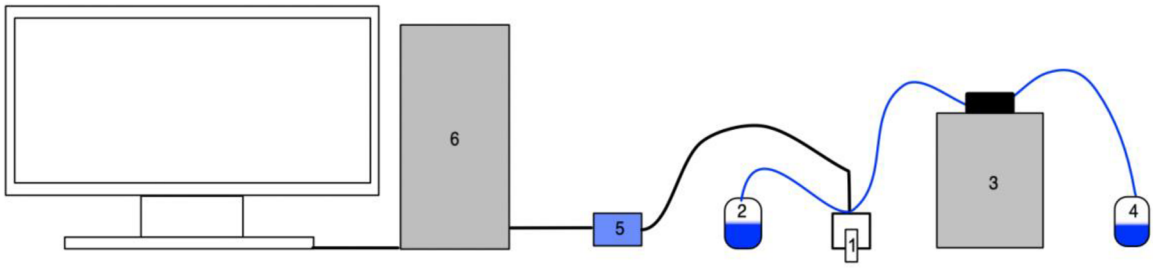

Figure 14 – Diagram of measuring apparatus.

1 – flow cell with ITO strip, 2 – beaker with a working solution, 3 – peristaltic pump, 4 – waste beaker, 5 – potentiostat, 6 - a desktop computer with PSTrace software

All measurements were performed at room temperature of 23 °C.

8.3.6 Cyclic voltammetry measurements

The cyclic voltammetry measurements were performed as follows: 1 µl of 1 mM ATCh (in PBS) and 1 µl of 1 mM $AgNO_3$ (in 5 mM phosphate) solutions were applied on the working electrode of AC1.W2.RS sensor with surface-immobilized AChE (1 nkat $µl^{-1}$). The mixture was incubated on the surface of the electrode for 5 minutes and then washed off with distilled water. Then the sensor was immersed in a beaker with PBS, and the CV measurement was performed using a potentiostat. The potential was set to 1 V with steps of 0.1 V.

The measurements using the inhibitor of AChE eserine were performed in the same manner, but before incubating the ATCh/$AgNO_3$ mixture, 1 µl of eserine aqueous solution (1 µg ml^{-1}, 5 µg ml^{-1}, 10 µg ml^{-1}, 20 µg ml^{-1}, 25 µg ml^{-1}) was applied to the working electrode and incubated for 5 minutes. After that, the inhibitor was washed off with distilled water. Followed the incubation of 1 µl of 1 mM ATCh (in PBS) and 1 µl of 1 mM $AgNO_3$ (in 5 mM phosphate) solutions. The mixture was left on the surface of the electrode for 5 minutes and then washed off with distilled water. Then the sensor was immersed in a beaker with PBS, and the CV measurement was performed using a potentiostat. The potential was set to 1 V with steps of 0.1 V. All measurements were performed at room temperature of 23 °C.

8.3.7 Spectrophotometric measurements

All spectrophotometric were performed in a cuvette with 10 mm pathlength using NanoPhotometer® NP 80. Absorption spectra were measured for citrate-capped AgNPs, a mixture of citrate-capped AgNPs with 1 mM ATCh (final concentration in the cuvette), a mixture of citrate-capped AgNPs with 1 mM ATCh and AChE (1 nkat μl^{-1}), and a mixture of citrate-capped AgNPs with 1mM ATCh and AChE (1 nkat μl^{-1}) and the inhibitor eserine (final concentration in the cuvette was 1 µg μl^{-1}).

In each measurement, the total volume of the solution in the cuvette was 1 ml. The mixture of 10 µl of ATCh and 10 µl of AChE was preincubated for 5 minutes before adding 980 µl of citrate-capped AgNPs. The same time of preincubation was applied for the mixture of 10 µl of ATCh, 10 µl of AChE, and 10 µl of eserine (final concentration in the cuvette was 10 µg μl^{-1}), which was then topped with 970 µl of citrate-capped AgNPs.

Wavescan mode was selected on the device, and the respective absorption spectra were measured.

8.3.8 AFM analysis of citrate-capped AgNPs

The AFM analysis was used to determine the size of prepared citrate-capped AgNPs and citrate-capped AgNPs aggregated by thiocholine (TCh).

For the analysis, the citrate-capped AgNPs were diluted 100 times with PBS. Then, the AgNPs were immobilized on AFM mica sheets using 10µM polylysine. Finally, the analysis itself was performed using the AFM Dimension FastScan Bio with Scanasyst-Air probes by Mgr. Matěj Pastucha.

The obtained images were processed using NanoScope Analysis software.

8.3.9 Raman spectroscopy analysis of citrate-capped AgNPs

The detection of traces of substances by surface-sensitive techniques such as surface-enhanced Raman spectroscopy (SERS) explores the interaction of adsorbed molecules on plasmonic surfaces to improve the limit of detection of analytes. [15] SERS is ultrasensitive vibrational spectroscopy that uses metal nanoparticles for

electromagnetic enhancement called localized surface plasmon resonance (LSPR) to enhance the Raman intensity of molecules. SERS is capable of recognizing various chemical substances in the mixture without the need to separate them. [27]

Surface-enhanced Raman scattering was another method used to determine the difference between fresh citrate-capped AgNPs and citrate-capped AgNPs aggregated by TCh. For this method, 10 µl of AgNP solution was first mixed with 4-mercaptobenzoic acid (1.2 mg ml^{-1}), and the mixed drop was allowed to dry on a slide with an aluminum foil layer. All Raman spectroscopy measurements were performed by Ing. Jakub Máčala.

9 Results and discussion

9.1 Results of amperometric measurements with platinum electrodes

To determine the amperometric response on AC1.W2.RS platinum sensors with surface-immobilized AChE of different activities, the sensors were immersed in a beaker with stirred (300 rpm) PBS solution (see 8.3.5), and the chronoamperometry method was selected in PSTrace software. The working potential was set to 300 mV.

Four volumes of 10 µl, 20 µl, 20 µl and 50 µl of 100mM ATCh solution were added sequentially into the beaker with PBS. These steps were repeated for all three activities of AChE (see 8.3.5; Figures 15-18). It was necessary to wait for a signal stabilization between each addition.

Each addition is marked with an arrow in graphs. In addition, a control measurement with an empty electrode was performed to determine a response to ATCh itself, as it might become slowly hydrolyzed spontaneously (Figure 19).

The current values in the following tables resemble the difference between two stabilized signals, i.e., they do not resemble the difference between each stabilized signal and the baseline signal. The total current value is a difference between the stabilized baseline signal and the highest stabilized signal.

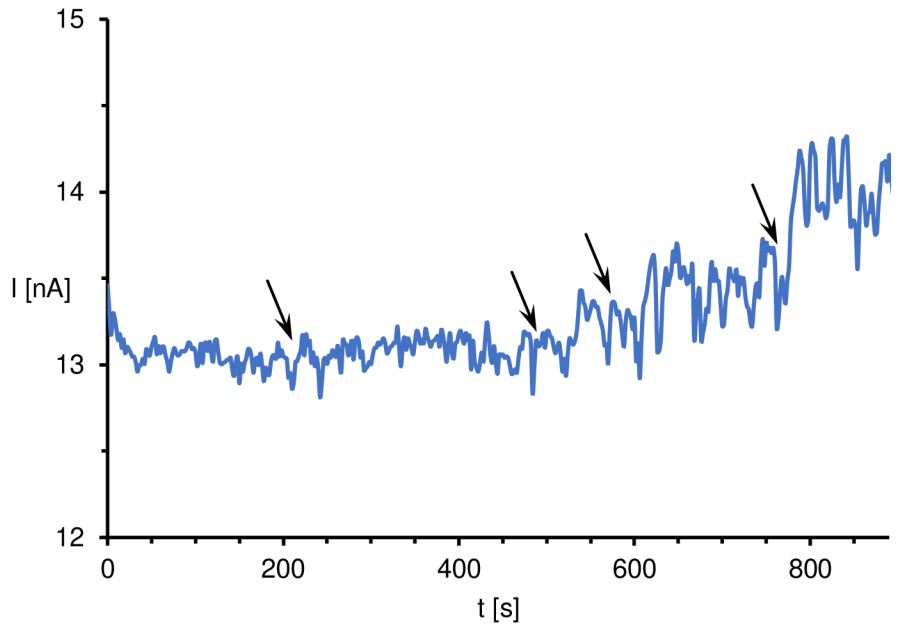

Figure 15 – Amperometric response to ATCh.

Pt-electrode with AChE (0.01 nkat μl^{-1}).

Table I – Responses to additions of ATCh (AChE 0.01 nkat μl^{-1}).

Time [s]	Addition of 100 mM ATCh [µl]	Final concentration [mM]	I [nA]	I (total) [nA]
240	10	0.1	0	
500	20	0.3	0.214	1.021
600	20	0.5	0.163	
780	50	1	0.644	

The missing response signal to the first addition of ATCh was most likely due to a combination of low concentration of ATCh and low activity of the immobilized enzyme.

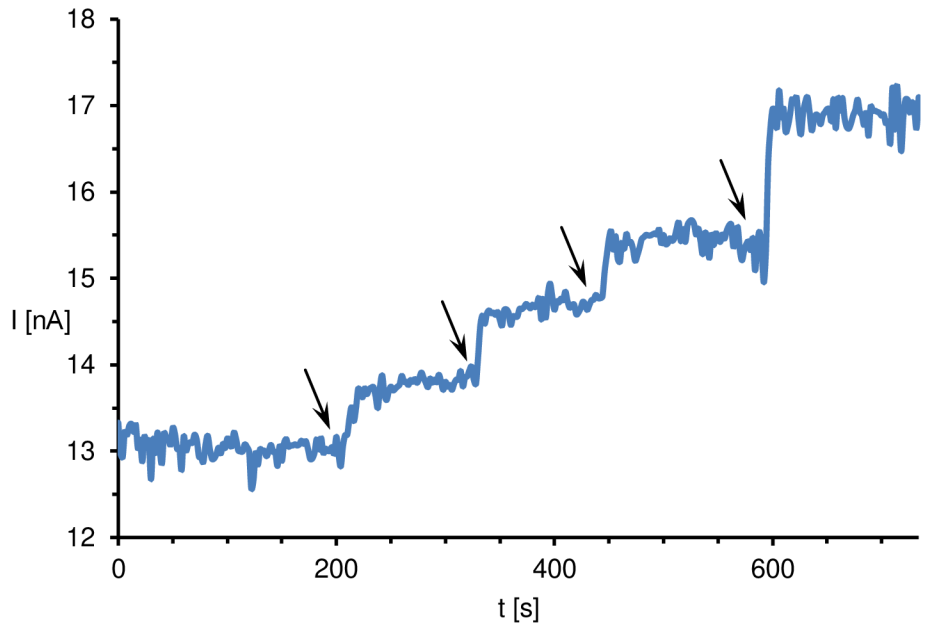

Figure 16 – Amperometric response to ATCh.

Pt-electrode with AChE (0.1 nkat μl^{-1}).

Table II – Responses to additions of ATCh (AChE 0.1 nkat μl^{-1}).

Time [s]	Addition of 100 mM ATCh [µl]	Final concentration [mM]	I [nA]	I (total) [nA]
220	10	0.1	0.75	3.854
340	20	0.3	0.848	
440	20	0.5	0.846	
600	50	1	1.41	

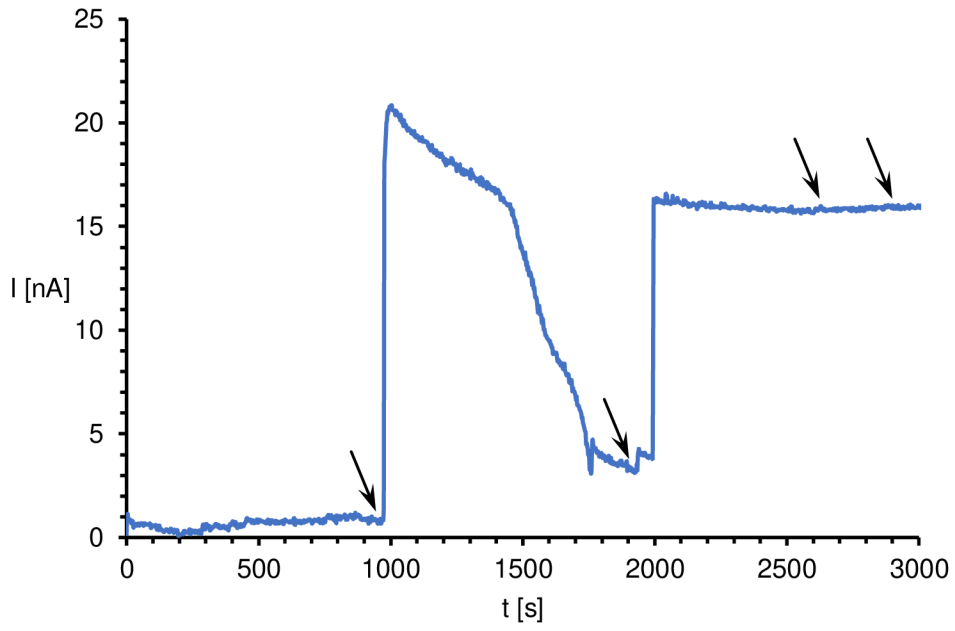

Figure 17 – Amperometric response to ATCh.

Pt-electrode with AChE (1 nkat μl^{-1}).

Table III – Responses to additions of ATCh (AChE 1 nkat μl^{-1}).

Time [s]	Addition of 100 mM ATCh [µl]	Final concentration [mM]	I [nA]	I (total) [nA]
950	10	0.1	2.538	16.143
1950	20	0.3	13.605	
2700	20	0.5	–	
2900	50	1	–	

As Figure 17 shows, no response signals were recorded for the last two additions of 20 µl and 50 µl of ATCh. That might be due to the fact that AChE is inhibited at high substrate concentrations. [28] In addition, the high concentrations of thiols – the produced thiocholine – might degrade the silver reference electrode surface.

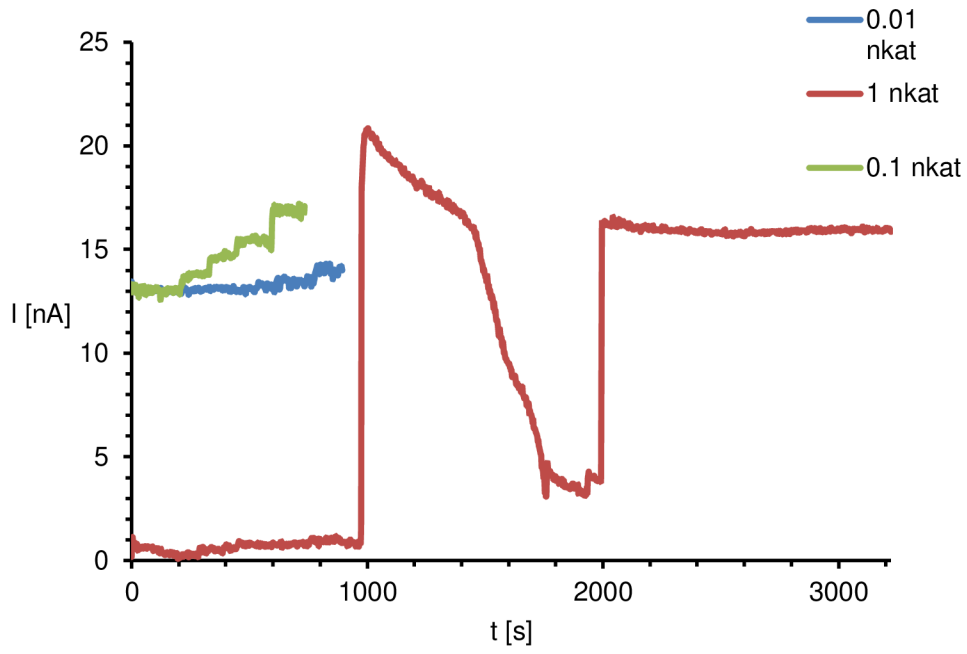

Figure 18 – Amperometric responses to ATCh all in one graph.

It is evident from Figure 18 that the response on the sensor with surface-immobilized AChE with an activity of 1 nkat μl^{-1} was the highest.

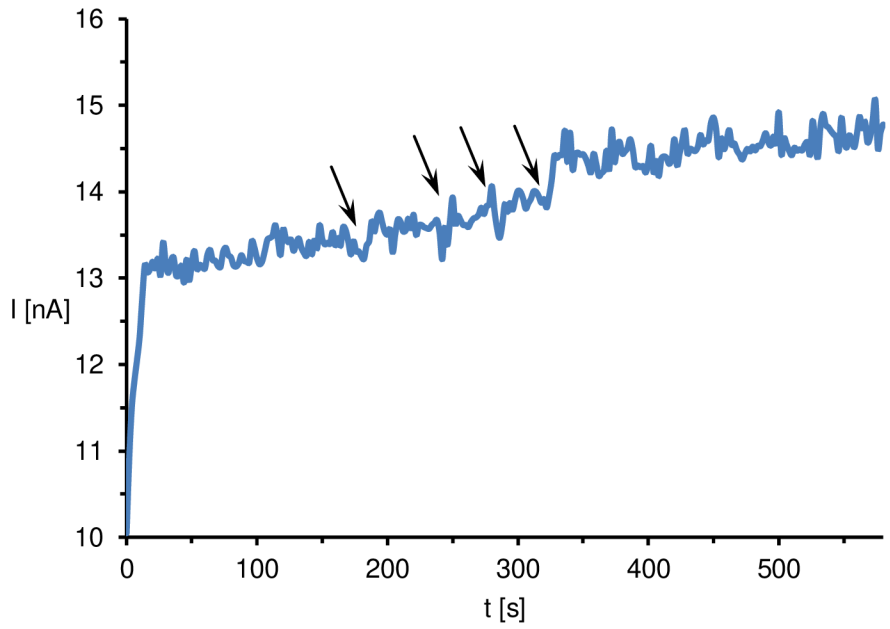

Figure 19 – Amperometric responses ATCh on an electrode without immobilized enzyme (control).

On the other hand, the total response to ATCh additions on an empty electrode was 1.1 nA, which is similar to the response on the sensor with surface-immobilized AChE with an activity of 0.01 nkat μl^{-1}.

Based on the obtained results, it was decided that all the other oncoming measurements with platinum electrodes were going to be performed using AChE with an activity of 1 nkat μl^{-1} and 1 mM ATCh. AC1.W2.RS platinum sensors have proven to be suitable for AChE immobilization and further measurements with ATCh.

9.2 Results of amperometric measurements with ITO strips

For the measurements of the amperometric response on ITO strips with surface-immobilized AChE, the strips were placed into a flow cell connected to the potentiostat, and the chronoamperometry method was selected in PSTrace software.

First, PBS was pumped into the cell, and after the signal stabilization, 1mM ATCh was pumped into the cell. Then, after the stabilization of the signal, PBS was pumped into the cell again. These steps were repeated for all measurements (see 8.3.5).

ATCh addition is marked with an arrow in each graph. In addition, a control measurement with an empty ITO was performed to determine a response to ATCh itself.

The current values in the following tables resemble the difference between the baseline signal of PBS and stabilized response signal to ATCh addition.

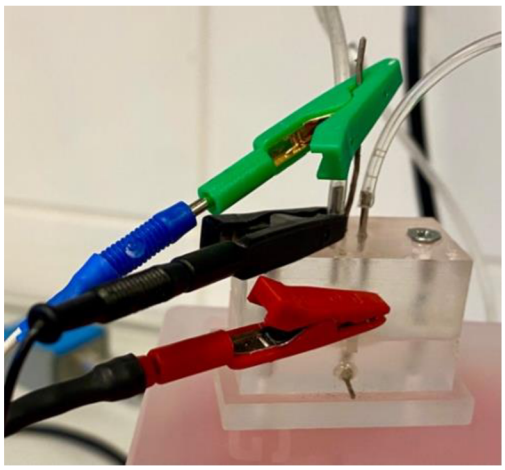

Figure 20 – Connection of the flow cell using crocodile clips.

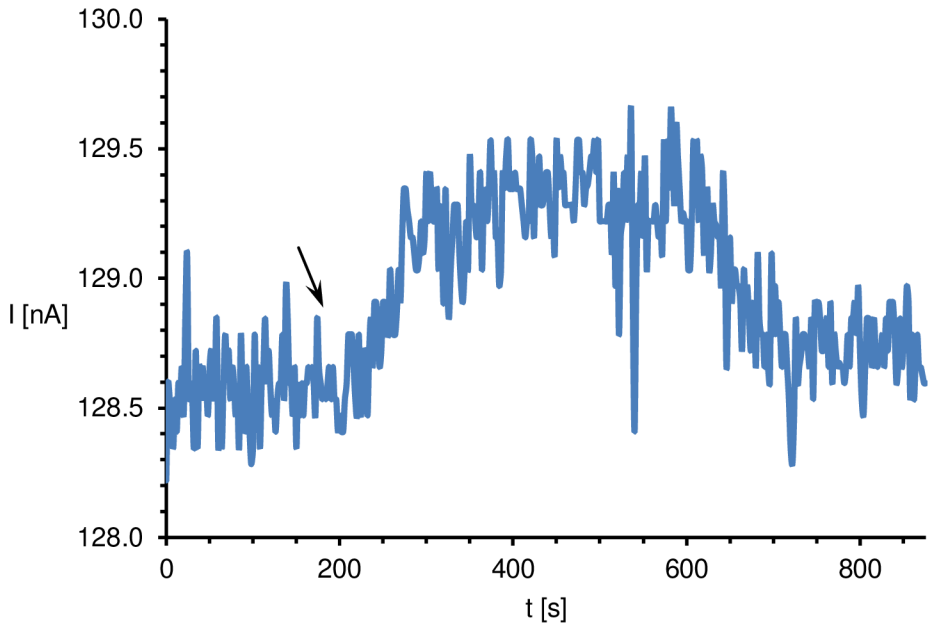

Figure 21 – Amperometric response to an addition of 1 mM ATCh on an ITO strip with surface-immobilized AChE (1 nkat μl^{-1}). Potential 600 mV.

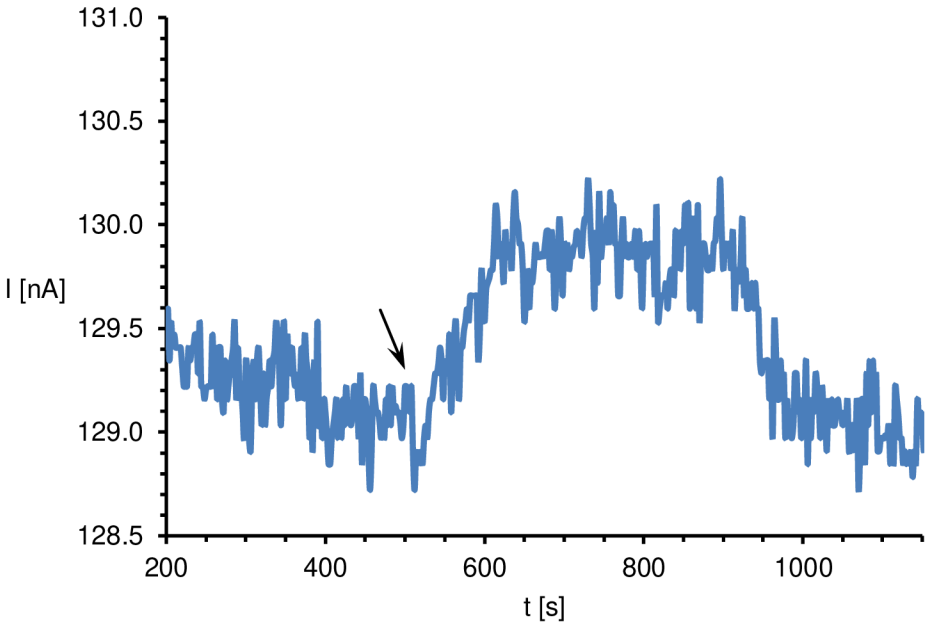

Figure 22 – Amperometric response to an addition of 1 mM ATCh on an ITO strip with surface-immobilized AChE (1 nkat μl^{-1}). Potential 700 mV.

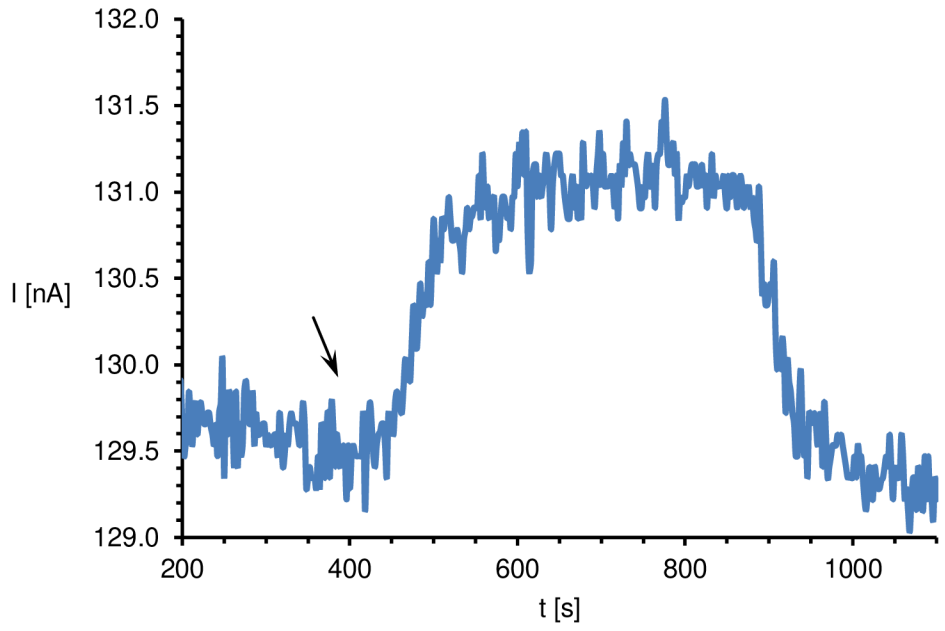

Figure 23 – Amperometric response to an addition of 1 mM ATCh on an ITO strip with surface-immobilized AChE (1 nkat μl^{-1}). Potential 800 mV.

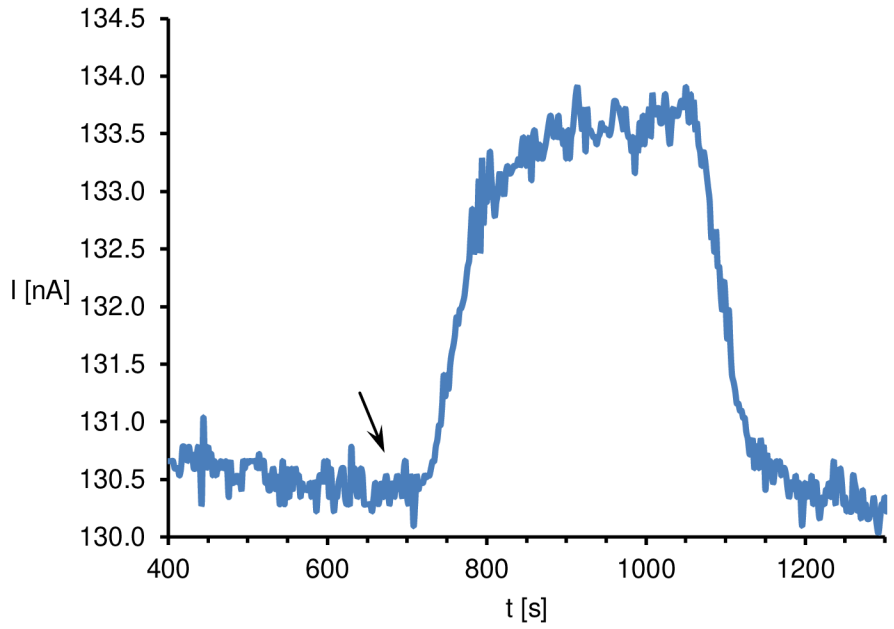

Figure 24 – Amperometric response to an addition of 1 mM ATCh on an ITO strip with surface-immobilized AChE (1 nkat μl^{-1}). Potential 1000 mV.

Table IV – Responses to additions of ATCh (AChE 1 nkat μl^{-1}).

E [mV]	600	700	800	1000
I [nA]	0.778	0.836	1.596	3.129

Based on the obtained results (Table IV), it is evident that the amperometric signal response was stronger at a higher potential. However, higher potentials can cause an unwanted interference of other compounds present in the system.

For the ITO strips with surface-immobilized AChE with an activity of 0.1 nkat μl^{-1} and 0.01 nkat μl^{-1}, it was only managed to record response signals at 800 mV.

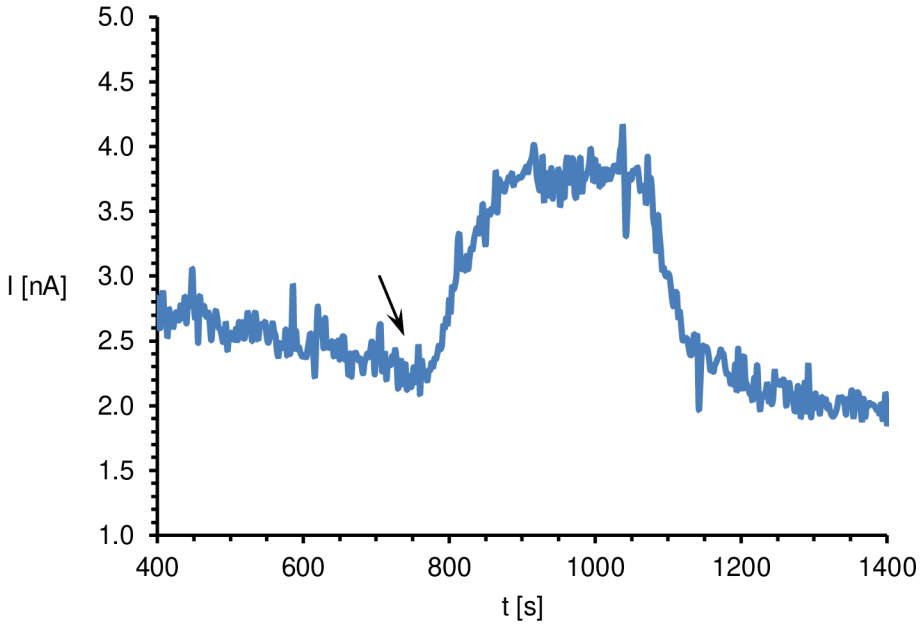

Figure 25 – Amperometric response to an addition of 1 mM ATCh on an ITO strip with surface-immobilized AChE (0.1 nkat μl^{-1}). Potential 800 mV.

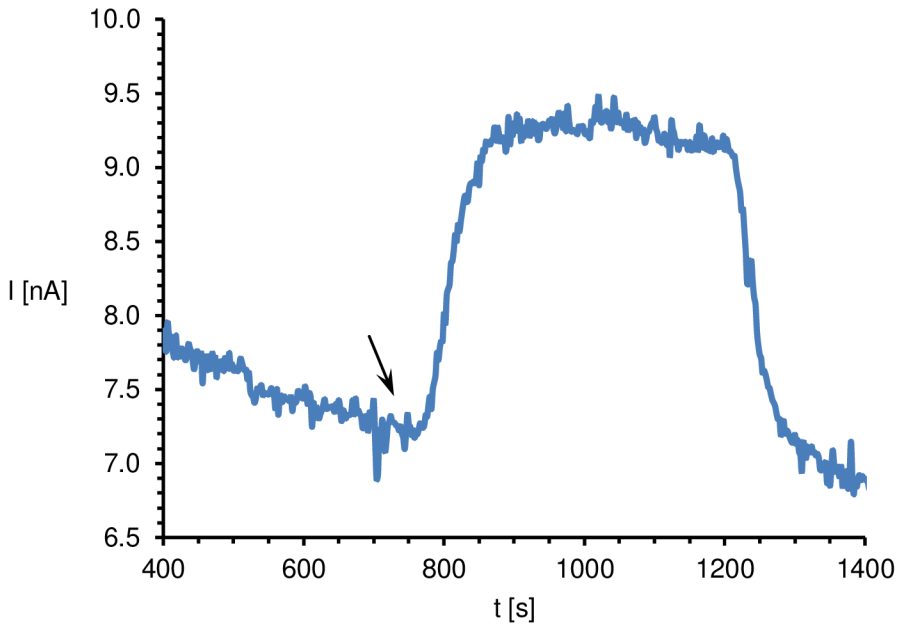

Figure 26 – Amperometric response to an addition of 1mM ATCh on an ITO strip with surface-immobilized AChE (0.01 nkat μl^{-1}). Potential 800 mV.

Table V – Responses to additions of ATCh.

	AChE 0.1 nkat μl^{-1}		**AChE 0.01 nkat μl^{-1}**	
E [mV]	600	800	600	800
I [nA]	0.778	0.836	1.596	3.129

On an empty ITO strip, no signal response was recorded. Although ITO strips with surface-immobilized AChE showed some amperometric response, the same results could not be achieved again when trying to replicate the experiments. Many ITO strips with the same activity of immobilized AChE showed no amperometric response. It seems that the bond between AChE and the silanized surface of ITO strips is very weak, and the enzyme is flushed from the surface by the addition of PBS into the flow cell.

For these reasons and lack of time, other planned ITO experiments had to be discontinued. So instead, attention was turned to platinum electrodes.

9.3 CV measurements with platinum electrodes

CV was another electrochemical method used to determine the response signals to ATCh on AChE immobilized platinum electrodes. It was also used to determine the change in signal response when inhibitor eserine was incubated on the surface of the sensor prior to the addition of ATCh.

All measurements were performed according to the above-described method (see 8.3.6). For the inhibition analysis, it was essential to wash off the inhibitor before applying the ATCh/$AgNO_3$ mixture to the working electrode.

The first experiment aimed to determine whether there was a difference in response to ATCh/$AgNO_3$ mixture on an empty sensor, a sensor with inhibited AChE (eserine 10 µg ml^{-1}), and a difference in preincubation times of the ATCh/$AgNO_3$ mixture (5 and 10 minutes) on sensors with uninhibited AChE. It was expected that the AgNPs generated in the solution would adhere to the surface of the electrode and provide an anodic signal on CVs.

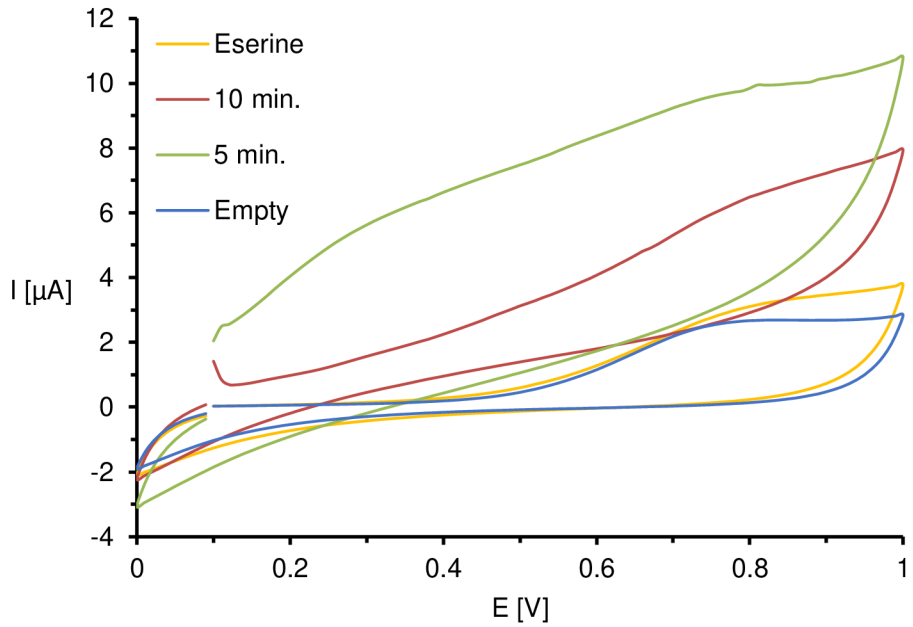

Figure 27 – CV response to ATCh/$AgNO_3$ mixture.

It can be seen in Figure 27 that the responses on the empty sensor and the sensor with inhibited AChE are very similar. Thus, it can be said that the inhibition took place on the surface of the electrode. As for the difference in incubation time, the signal response after 5 minutes of incubation was higher. Hence, all the other incubations were carried out for 5 minutes.

The second CV experiment was set to determine whether there is a difference in signal responses for various concentrations of eserine. The selected concentrations of eserine were 1 µg ml^{-1}, 5 µg ml^{-1}, 10 µg ml^{-1}, 20 µg ml^{-1}, and 25 µg ml^{-1}. A drop of inhibitor was first incubated on the surface of the electrode for 5 minutes, then washed off. Then the ATCh/$AgNO_3$ mixture was incubated on the surface for another 5 minutes before being washed off.

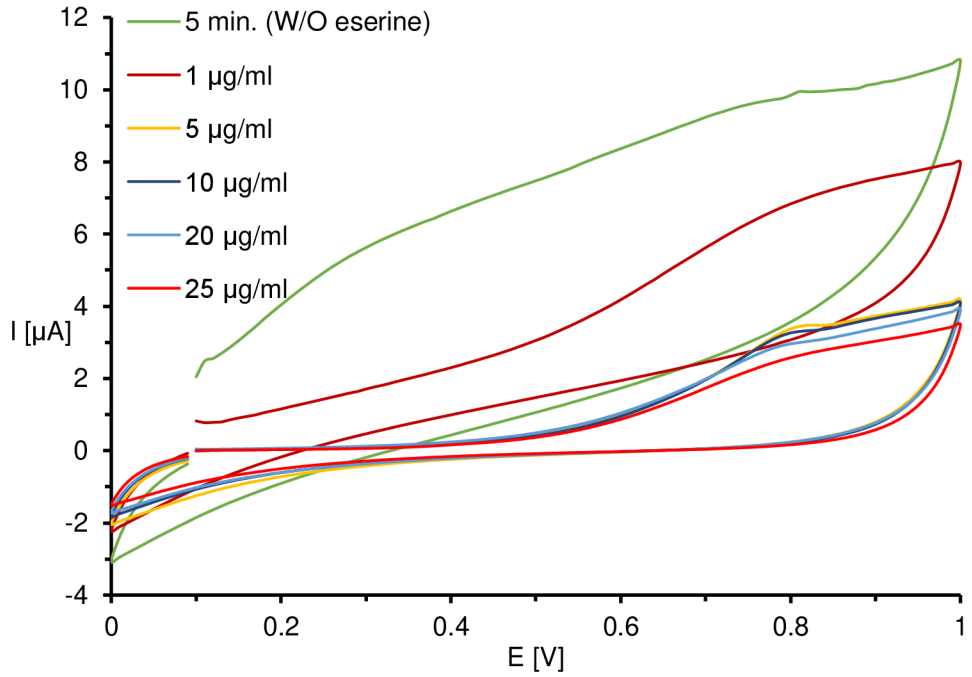

Figure 28 – CV response to ATCh/$AgNO_3$ mixture (various inhibitor concentrations).

It is evident from Figure 28 that with increasing concentration of inhibitor, the signal response decreased. Thus, there is a dependence between the concentration of inhibitor and voltammetric response intensity. For comparison, the curve for 5-minute incubation without eserine was added to the graph to demonstrate that even at 1 µg ml^{-1} of eserine, some inhibition took place.

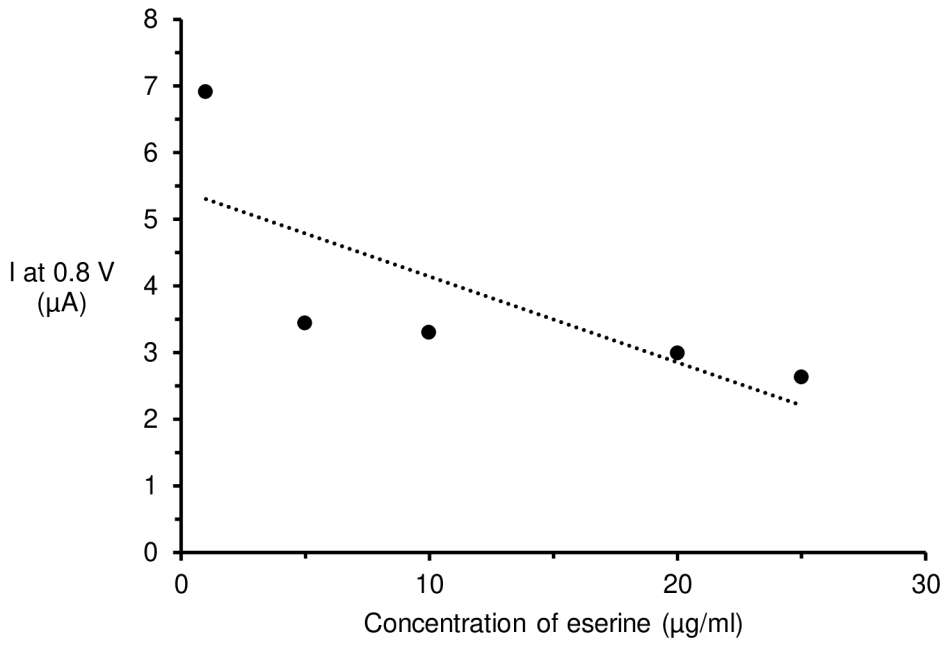

Figure 29 – Current at 0.8 V (top half-wave) against eserine concentrations.

Figure 29 shows the decreasing trend of current with increasing inhibitor concentration. For this graph, the current values at 0.8 V of the upper half-wave were used.

CV combined with platinum electrodes with surface-immobilized AChE seems to be a promising method for the determination of the inhibitors of AChE.

9.4 Spectrophotometric measurements of citrate-capped AgNPs

Citrate-capped AgNPs were used for spectrophotometric determination of the inhibition of AChE. AgNPs prepared with both sodium and potassium citrate were used for this experiment. This experiment was based on the work of Z. Li et al. [16]

AChE hydrolyzes ATCh to acetic acid and thiocholine, which induces aggregation of AgNPs, leading to color change from yellow to red-brown (Figures 30 and 31). The absorption maximum of AgNPs lies around 400 nm.

The analyzed solutions were prepared according to the above-described method (see 8.3.7).

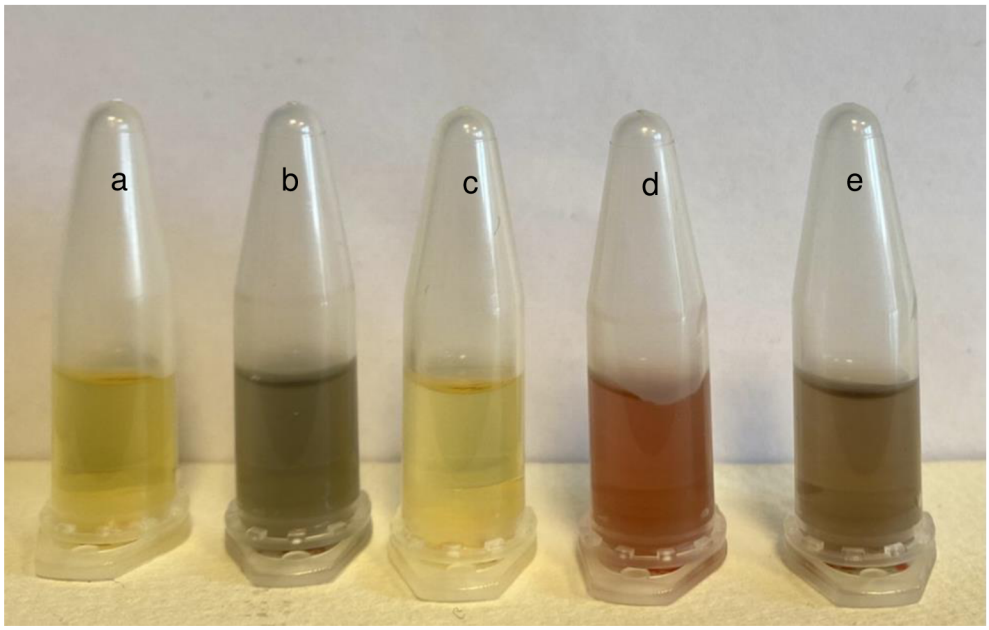

Figure 30 – Citrate-capped AgNPs prepared using sodium citrate.

a – AgNPs, b – AgNPs + ATCh, c – AgNPs + AChE, d – AgNPs + AChE + ATCh, e – AgNPs + AChE + ATCh + eserine

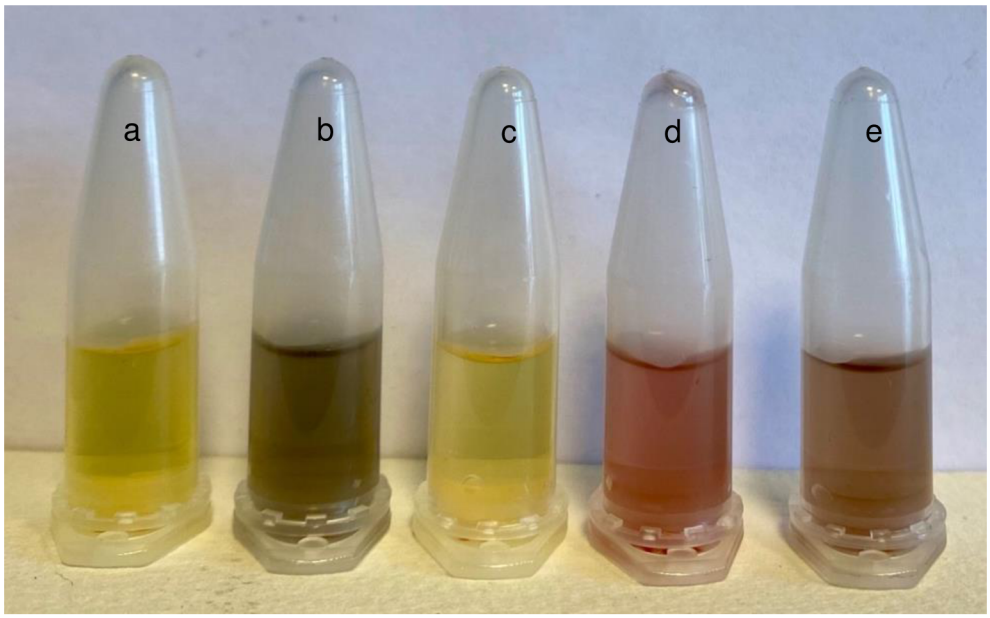

Figure 31 – Citrate-capped AgNPs prepared using potassium citrate.

a – AgNPs, b – AgNPs + ATCh, c – AgNPs + AChE, d – AgNPs + AChE + ATCh, e – AgNPs + AChE + ATCh + eserine

UV-VIS spectra were recorded for the solutions in the pictures above. Ideally, the mixture of AgNPs and ATCh should not undergo any color change. However, due to the fast self-dissociation of ATCh, it was hard to avoid oxidation of the mixture. On the other hand, the color change from yellow to red-brown caused by the TCh-induced aggregation of AgNPs is evident in both pictures. There was also a slight color change in the inhibited samples. Nevertheless, again the self-dissociation of ATCh made it hard to distinguish between the sample containing just AgNPs and ATCh and the inhibited sample.

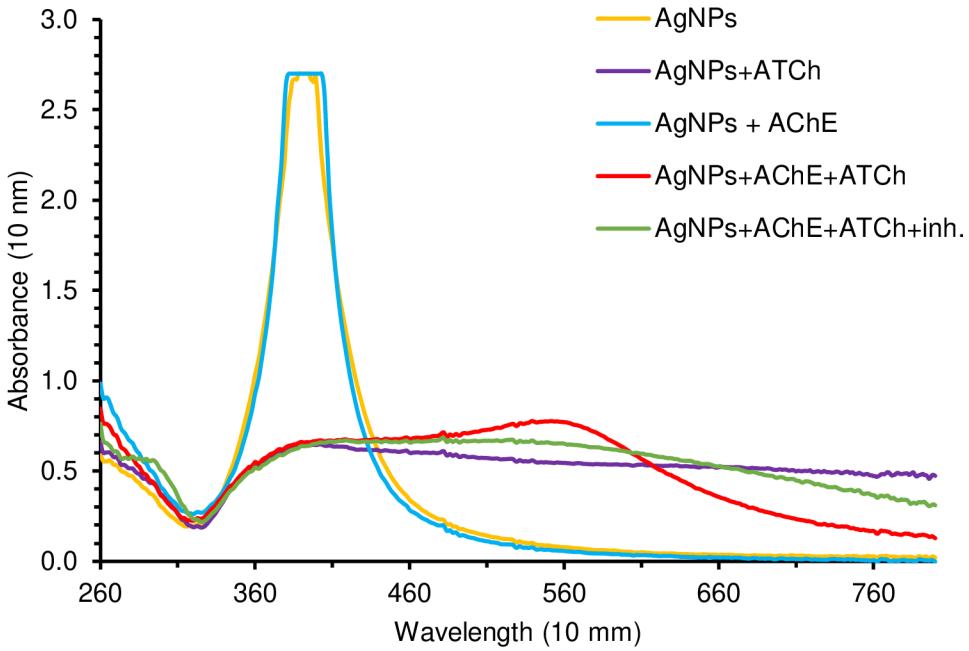

Figure 32 – Recorded spectra for solutions prepared using AgNPs prepared with sodium citrate.

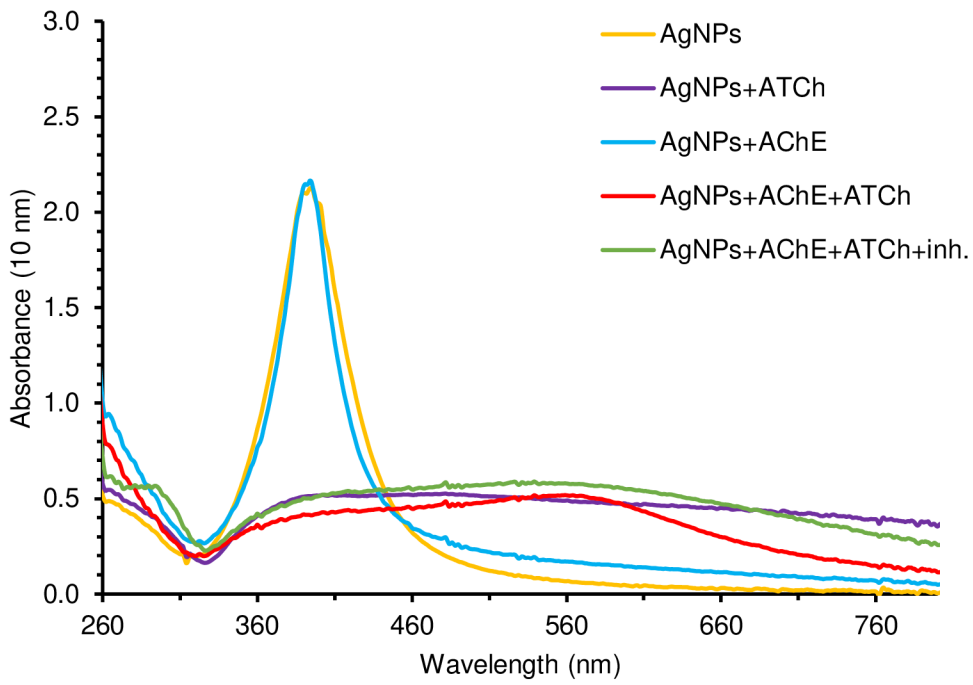

Figure 33 – Recorded spectra for solutions prepared using AgNPs prepared with potassium citrate.

In both cases, there is an absorption maximum peak at about 400 nm for AgNPs and AgNPs with AChE. Also, a broad absorption band at about 520 nM can be observed in Figures 32 and 33, indicating the color change from yellow to red-brown caused by TCh.

Ideally, the maximum peaks at 400 nm should be similar for all the mixtures except the one containing the inhibitor and the one where the AChE-mediated hydrolysis of ATCh caused the color change from yellow to red-brown.

Although promising, this method would require further investigation on how to avoid the self-dissociation of ATCh and the oxidation of AgNPs associated with that.

9.5 AFM

The AFM analysis was used to determine the size of prepared AgNPs and the size of AgNPs aggregated by TCh. For this purpose, the same solutions of pure AgNPs and AgNPs aggregated by TCh as in the spectrophotometric analysis were used. The samples were prepared according to the above-described method (see 8.3.8).

The size of analyzed fresh nanoparticles varied from 2 to 20 nm. The size of aggregated AgNPs was around 60 nm. Figures 34-37 show the AFM images of prepared AgNPs and aggregates thereof.

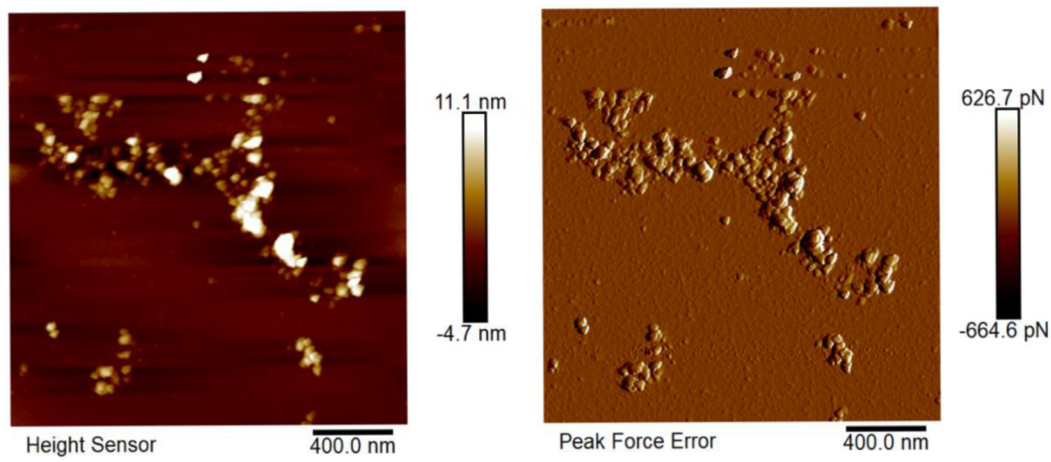

Figure 34 – AFM images of citrate-capped AgNPs (sodium citrate).

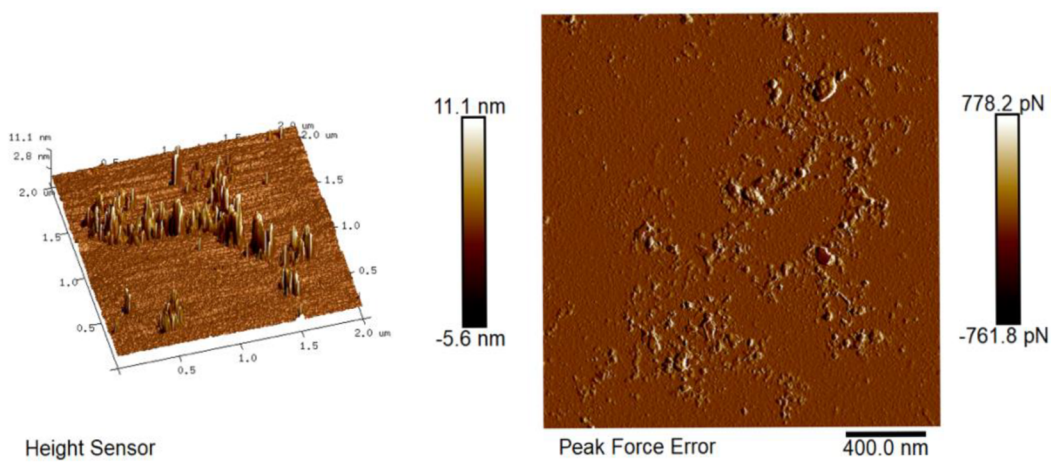

Figure 35 – AFM images of citrate-capped AgNPs (sodium citrate).

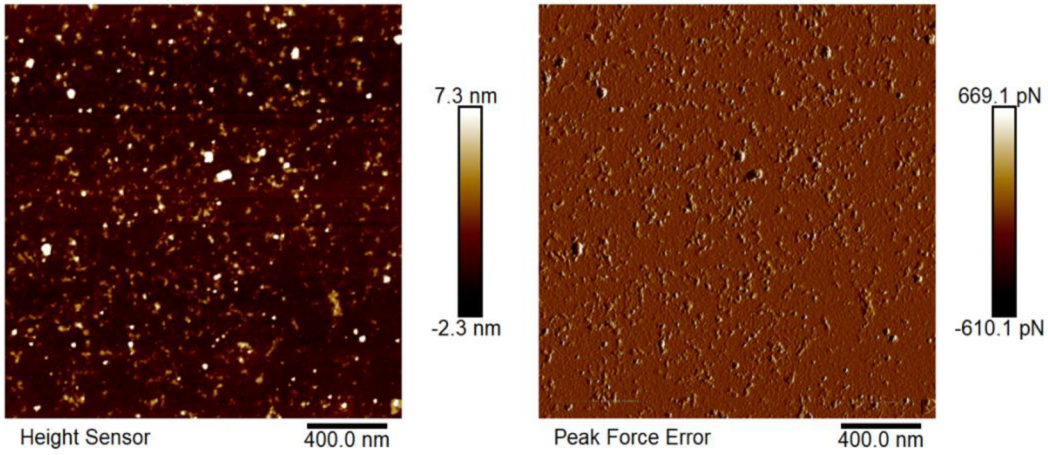

Figure 36 – AFM images of citrate-capped AgNPs (potassium citrate).

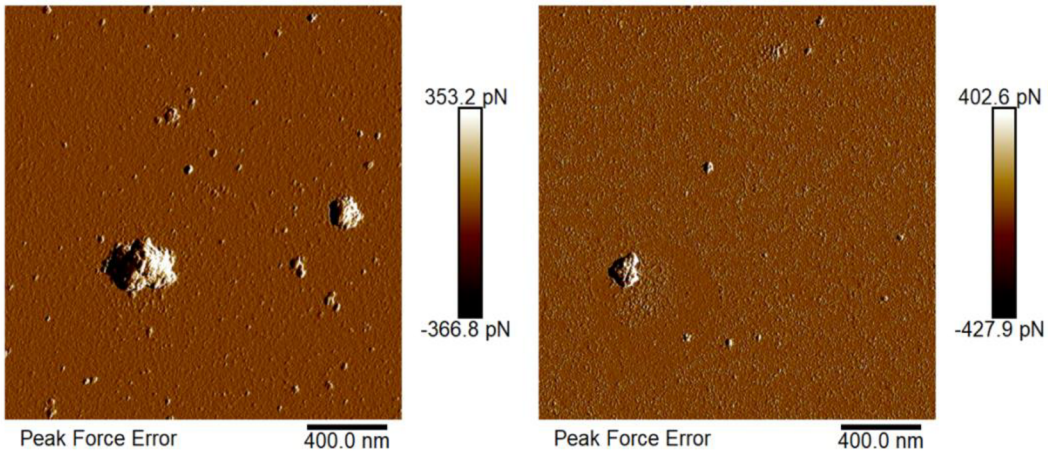

Figure 37 – AFM images of aggregated AgNPs (potassium citrate – left, sodium citrate – right).

Thanks to the AFM imaging, it was possible to determine the size of prepared AgNPs and to confirm the formation of AgNP aggregates induced by TCh. It was affirmed that in the absence of thiols from TCh, the AgNPs were smaller and spread evenly, whereas, in the presence of thiols from TCh, they became larger, aggregated, and less evenly spread.[12] Furthermore, as starting material, the potassium citrate-based AgNPs seemed to be more homogeneous, which is an advantage.

Further AFM analyses would have been targeted to compare TCh-aggregated AgNPs and samples where the hydrolysis of ATCh was inhibited.

9.6 Raman spectroscopy

Raman spectroscopy was also used to determine the difference between fresh and aggregated AgNPs. For this method, 4-MBA was used as a reporter molecule to functionalize the AgNPs for SERS.

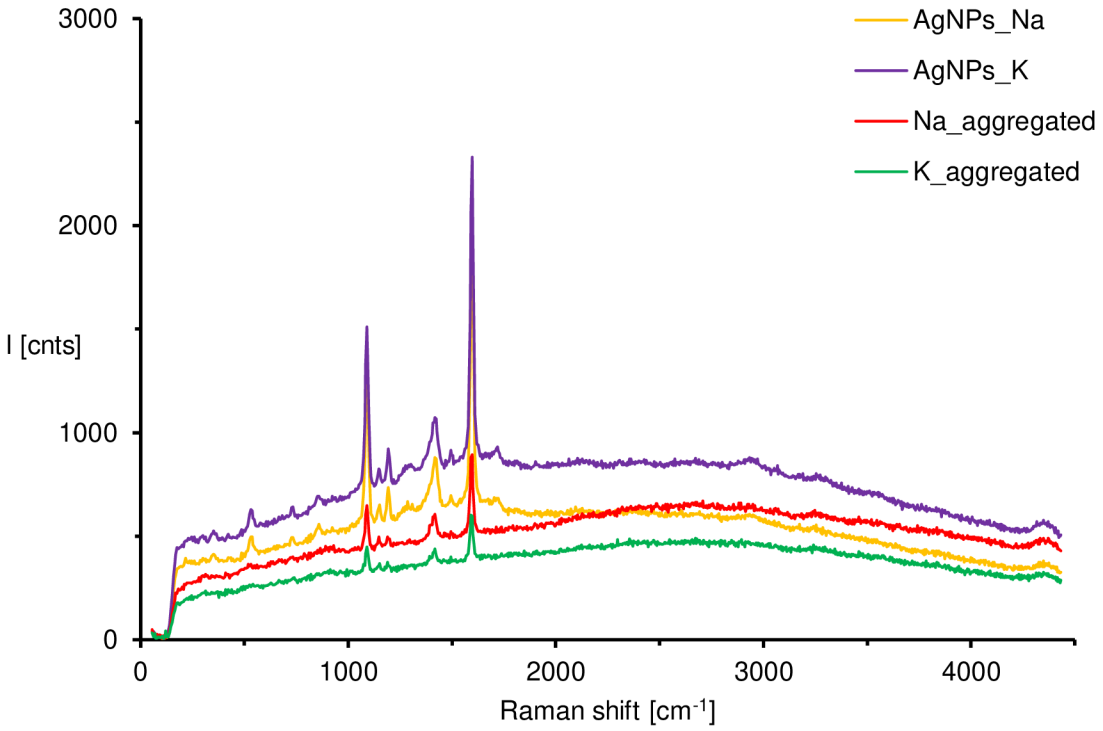

Figure 38 – SERS of fresh and aggregated AgNPs.

The recorded SERS spectra (Figure 38) show decreased intensity for AgNPs aggregated by TCh (green and red curves).

Table VI – Intensity at 1590 cm^{-1}.

	I [cnts] at 1590 cm^{-1}	
Fresh AgNPs	2057 (Na)	2331 (K)
Aggregated AgNPs	894 (Na)	596 (K)

The peak intensity values at 1590 cm^{-1} were 2057 cnts (prepared with sodium citrate) and 2331 cnts (prepared with potassium citrate) for the fresh AgNPs and 894 cnts (Na) and 596 cnts (K) for the aggregated AgNPs. Thus, the difference in peak intensity indicates a size difference between the fresh and aggregated AgNPs.

Thanks to the ability to distinguish between the fresh and aggregated AgNPs, Raman spectroscopy could serve well for the indication of AChE inhibition. When analyzing a mixture of AChE, ATCh, and citrate-capped AgNPs, there should be an observable difference in intensity when an inhibitor blocking the AChE-mediated hydrolysis of ATCh is present in the mixture – no or fewer AgNP aggregates should be present in the mixture. On the other hand, when the inhibitor is not present in the mixture, TCh should induce the formation of AgNP aggregates.

Using SERS for this purpose also requires further investigation.

10 Conclusion

Amperometric and CV measurements, with sensors with surface-immobilized AChE and ATCh as a model substrate, were performed in the practical part of this thesis. Unfortunately, some of the experiments could not be replicated. Hence, the results remain unclear. The measurements were carried out in a stirred arrangement and a flow cell. It was managed to record differences in response signals for AChE inhibition caused by various concentrations of inhibitor eserine.

Further, citrate-capped AgNPs were prepared. These AgNPs were used in spectrophotometric determination of AgNP aggregation caused by TCh and the inhibition of AChE caused by eserine.

The size of prepared citrate-capped AgNPs and the aggregates thereof was determined using AFM analysis. In addition, surface-enhanced Raman Spectroscopy was also used to determine the difference in physical properties of fresh and aggregated AgNPs.

Creating a robust electrochemical system for detecting AChE inhibitors using AgNPs as signal enhancers is likely possible given more research time.

11 Bibliography

[1] M. B. Colović, D. Z. Krstić, T. D. Lazarević-Pašti, A. M. Bondžić, and V. M. Vasić, "Acetylcholinesterase inhibitors: pharmacology and toxicology," *Curr Neuropharmacol*, vol. 11, no. 3, pp. 315–335, May 2013, doi: 10.2174/1570159X11311030006.

[2] "NATIVE ACETYLCHOLINESTERASE (E.C. 3.1.1.7) FROM TORPEDO CALIFORNICA." May 2021. Accessed: May 15, 2021. [Online]. Available: https://www.rcsb.org/structure/2ACE

[3] A. Trang and P. B. Khandhar, "Physiology, Acetylcholinesterase.," in *StatPearls*, Treasure Island (FL): StatPearls Publishing, 2021.

[4] "ELECTROPHORUS ELECTRICUS ACETYLCHOLINESTERASE." Accessed: May 15, 2021. [Online]. Available: https://www.rcsb.org/structure/1C2B

[5] M. G. Lionetto, R. Caricato, A. Calisi, M. E. Giordano, and T. Schettino, "Acetylcholinesterase as a biomarker in environmental and occupational medicine: new insights and future perspectives," *Biomed Res Int*, vol. 2013, pp. 321213–321213, Jul. 2013, doi: 10.1155/2013/321213.

[6] E. Fajemisin, O. Bamidele, S. Ogunsola, and A. Aiyenuro, "The Organ Distribution, Characterization and Modification of Acetylcholinesterase Activity in Adult African Grasshopper: Zonocerus sp Linn.," *Asian Journal of Research in Biochemistry*, pp. 1–9, Nov. 2019, doi: 10.9734/ajrb/2019/v5i430097.

[7] J. Ž. Karasová, K. Kuča, D. Jun, and J. Bajgar, "UŽITÍ ELLMANOVY METODY PRO STANOVENÍ AKTIVIT CHOLIN- ESTERAS PŘI IN VIVO HODNOCENÍ ÚČINKŮ REAKTIVÁTORŮ," *Chem. Listy*, vol. 104, no. 1, pp. 46–50, Feb. 2010.

[8] K. Vrchovecká, "Nanočástice kovů pro zvýšení signálu biosensorů [online].," Bachelor's thesis, Masarykova univerzita, Brno, 2015. Accessed: May 07, 2021. [Online]. Available: https://is.muni.cz/th/i52pd/

[9] J. Weller and A. Budson, “Current understanding of Alzheimer’s disease diagnosis and treatment,” *F1000Res*, vol. 7, p. F1000 Faculty Rev-1161, Jul. 2018, doi: 10.12688/f1000research.14506.1.

[10] A. Vale and M. Lotti, “Organophosphorus and carbamate insecticide poisoning.,” *Handb Clin Neurol*, vol. 131, pp. 149–168, Nov. 2015, doi: 10.1016/B978-0-444-62627-1.00010-X.

[11] J. Bajgar, “Laboratory examination in nerve agent intoxication.,” *Acta Medica (Hradec Kralove)*, vol. 56, no. 3, pp. 89–96, Nov. 2013, doi: 10.14712/18059694.2014.15.

[12] D. Nanda Kumar, S. A. Alex, N. Chandrasekaran, and A. Mukherjee, “Acetylcholinesterase (AChE)-mediated immobilization of silver nanoparticles for the detection of organophosphorus pesticides,” *RSC Adv.*, vol. 6, no. 69, pp. 64769–64777, 2016, doi: 10.1039/C6RA13185A.

[13] Z. Liu, X. Xia, G. Zhou, L. Ge, and F. Li, “Acetylcholinesterase-catalyzed silver deposition for ultrasensitive electrochemical biosensing of organophosphorus pesticides,” *Analyst*, vol. 145, no. 6, pp. 2339–2344, Mar. 2020, doi: 10.1039/C9AN02546D.

[14] N. Chauhan and C. S. Pundir, “An amperometric acetylcholinesterase sensor based on Fe3O4 nanoparticle/multi-walled carbon nanotube-modified ITO-coated glass plate for the detection of pesticides,” *Electrochimica Acta*, vol. 67, pp. 79–86, Apr. 2012, doi: 10.1016/j.electacta.2012.02.012.

[15] J. M. Dias Soares and H. P. de Oliveira, “Silver-based surface enhanced Raman spectroscopy devices for detection of organophosphorus pesticides traces.,” *Biotechnol Prog*, vol. 35, no. 4, p. e2809, Jul. 2019, doi: 10.1002/btpr.2809.

[16] Z. Li, Y. Wang, Y. Ni, and S. Kokot, “Unmodified silver nanoparticles for rapid analysis of the organophosphorus pesticide, dipterex, often found in different waters,” *Sensors and Actuators B: Chemical*, vol. 193, pp. 205–211, Mar. 2014, doi: https://doi.org/10.1016/j.snb.2013.11.096.

[17] E. B. Aydın and M. K. Sezgintürk, “Indium tin oxide (ITO): A promising material in biosensing technology,” *TrAC Trends in Analytical Chemistry*, vol. 97, pp. 309–315, Dec. 2017, doi: 10.1016/j.trac.2017.09.021.

[18] T. Hlaváčová, “Fotoelektrochemické enzymové biosensory,” Diplomová práce, Masarykova univerzita, Brno, 2020. Accessed: May 14, 2021. [Online]. Available: https://is.muni.cz/th/oifv8/

[19] S. Elmas, Ş. Korkmaz, and S. Pat, “Optical characterization of deposited ITO thin films on glass and PET substrates,” *Applied Surface Science*, vol. 276, pp. 641–645, Jul. 2013, doi: 10.1016/j.apsusc.2013.03.146.

[20] G. A. Rechnitz, “Biosensors into the 1990s,” *Electroanalysis*, vol. 3, no. 2, pp. 73–76, 1991, doi: 10.1002/elan.1140030202.

[21] P. Skládal, “Biosensory.” Masarykova Univerzita, 2002.

[22] D. R. Thévenot, K. Toth, R. A. Durst, and G. S. Wilson, “Electrochemical biosensors: recommended definitions and classification1International Union of Pure and Applied Chemistry: Physical Chemistry Division, Commission I.7 (Biophysical Chemistry); Analytical Chemistry Division, Commission V.5 (Electroanalytical Chemistry).1,” *Biosensors and Bioelectronics*, vol. 16, no. 1, pp. 121–131, Jan. 2001, doi: 10.1016/S0956-5663(01)00115-4.

[23] M. Kronďák, “Clarkovo čidlo pro měření koncentrace rozpuštěného kyslíku,” *Vesmír*, vol. 89, no. 631, Oct. 2010. Accessed: Apr. 19, 2019. [Online]. Available: https://vesmir.cz/cz/casopis/archiv-casopisu/2010/cislo-10/clarkovo-cidlo-pro-mereni-koncentrace-rozpusteneho-kysliku.html

[24] A. Quiroga, “Cyclic Voltammetry,” Aug. 2020, Accessed: Apr. 25, 2021. [Online]. Available: https://chem.libretexts.org/@go/page/311

[25] Skoog, D. A., Holler, F. J., & Crouch, S. R. (2007). "Principles of instrumental analysis." Belmont, CA: Thomson Brooks/Cole.

[26] “Cyclic voltammetry.” Accessed: May 15, 2021. [Online]. Available: https://d4ceckwy45dem.cloudfront.net/wp-content/uploads/2017/12/voltammogram-600x505.png

[27] T. Sukmanee, K. Wongravee, S. Ekgasit, C. Thammacharoen, and P. Pienpinijtham, “Facile and Sensitive Detection of Carbofuran Carbamate Pesticide in Rice and Soybean Using Coupling Reaction-based Surface-Enhanced Raman Scattering.,” *Anal Sci*, vol. 33, no. 1, pp. 89–94, Jan. 2017, doi: 10.2116/analsci.33.89.

[28] J.-P. Colletier *et al.*, “Structural insights into substrate traffic and inhibition in acetylcholinesterase,” *EMBO J*, vol. 25, no. 12, pp. 2746–2756, Jun. 2006, doi: 10.1038/sj.emboj.7601175.